ICE FLOW MODELLING OF ICE SHELVES AND ICE CAPS

Yongmei Gong

ACADEMIC DISSERTATION IN GEOPHYSICS

To be presented, with the permission of the Faculty of Science of the University of Helsinki for public criticism in Auditorium CK112 of Exactum, Gustaf Hällströmin katu 2 b, on February 13rd, 2018, at 12 o´clock noon.

ISBN 978-951-51-4043-2 (paperback)
ISBN 978-951-51-4044-9 (PDF)
ISSN 0355-8630

Helsinki 2018
Unigrafia

Abstract

Ice shelves and ice caps constitute a great proportion of the glacial ice mass that covers 10% of the global land surface and is vulnerable to climate change. Large scale ice flow models are widely used to investigate the mechanisms behind the observed physical processes and predict their future stability and variability under climate change.

This thesis aims at providing general remarks on the application of ice flow models in studying glaciological problems through investigating the evolution of an Antarctic ice shelf under climate change and the mechanisms of fast ice flowing events (surges) in an Arctic ice cap. In addition discussions of the equivalence of two significantly different expressions for the rate factor in Glen's flow are also provided.

Off-line coupling between the Lambert Glacier-Amery Ice Shelf (LG-AIS) drainage system, East Antarctica, and the climate system by employing a hierarchy of models from general circulation models, through high resolution regional atmospheric and oceanic models, to a vertically integrated ice flow model has been carried out. The adaptive mesh refinement technique is specifically implemented for resolving the problem concerning grounding line migration. Sensitivity tests investigating the importance of various parameters and boundary conditions are carried out in ice flow models with different approximations for Austfonna Ice-cap, Svalbard to investigate the surge event in one of its basins, Basin 3. Inverse modelling of basal friction coefficient is specifically implemented. A continuum to discrete multi-model approach is implemented for simulations of Basin 3.

LG-AIS drainage system will be rather stable in the face of future warming over 21st and 22nd centuries. Although the ice shelf thins in most of the simulations there is little grounding line retreat. The change of ice thickness and velocity in the ice shelf is mainly influenced by the basal melt distribution. And the Lambert, Fisher and Mellor glaciers are most sensitive to thinning of the ice shelf south of Clemence Massif. The sea level rise contribution of LG-AIS is modest as the increased accumulation computed by the atmosphere models outweighs ice stream acceleration.

Using a temporally fixed basal friction field obtained through inverse modelling is insufficient to simulate the future changes of the fast flowing surging glacier in Basin 3. And the evolution of basal friction patterns, and in turn basal processes are among the most important factors during the surge in Basin 3. A system of processes and feedbacks involving till deformation and basal hydrology is more

likely to explain both the seasonal accelerations and the ongoing inter-annual speed-up more than a hard-bed mechanism.

The continuum to discrete multi-model approach provides the possible locations of the crevasses that can potentially cut through the full length of the ice and deliver surface melt water down to the bed. The calculated basal water flow paths according to hydraulic potential indicate that the summer speed up events and the initiation of the acceleration in the southern part of the basin can be explained by either a direct enhancement to the ice flow through basal lubrication or a lagged-in-time mechanism through the outflow of accumulated water in the over-deepening area.

Keywords: ice flow modelling, climate change, sea level rise, future projection, basal sliding, basal hydrology, surface melt, surging glacier, Lambert Glacier-Amery Ice Shelf, Austfonna Ice-cap, Antarctic, Svalbard

Acknowledgements

People have told me that a doctoral study is full of suffering. Since eventually I have survived it I would like to call it a sufferfest – "*An activity whereby all participants ache, agonize, ail, be at a disadvantage, be racked, deteriorate, endure, grieve, languish, and/or writhe.. but by co-misery, yet co-hesiveness, will have experienced a grand time. Often survived through sarcasm* (Sufferfest 1, 2014)". Thus I would like to thank all the people below for their guidance, support, entertainment, co-sufferance and everything that helped me coping with the suffering.

First of all, I would like to thank all the wise men I met on my way going through the mist of the 'research forest'. I thank Dr. Stephen Cornford, Dr. Rupert Gladstone, Prof. Matti Leppäranta, Prof. John Moor, Dr. Martina Schäfer, Dr. Thomas Zwinger and Dr. Jan Åström for inspiring me with their passion in glaciological research, for giving me advice on how to be a researcher and for tolerating my ignorance from the very beginning till the very end.

Secondly, I would like to thank all the allies who were there by my side when fighting in the 'research battle'. I thank all my collaborators and colleagues for providing data and discussion for my research and all the friendly and intelligent glaciologists, computer scientists, geophysicists, earth scientists etc. whom I met in conferences, workshops, summer schools and so on for sharing their knowledge and ideas and pushing me forward in my study. Their names cannot all be listed here as there are so many.

Thirdly, I would like to thank all my friends who laughed, cried, climbed, sang and danced with me when I was not absorbed in my scientific world and who have helped me surviving cold and dark winters in this foreign country with warm food, good beverages, happy music and silly jokes. I do not want to list their names here as I am afraid of missing single one of them. And they have been trying very hard to keep me outside of my research bubble so I will not put them in.

Then, of course, I would like to thank all my funders - Nordic Centre of Excellence SVALI, European Science Foundation, Väisälä Foundation and the doctoral program ATM-DP, Helsinki Univ. for their appreciation and generosity. Without them I would not have had the chance to go to all the magical places where glaciers are and this thesis would never have had existed. And also I thank CSC-IT centre for science for providing computational facilities and support on Elmer/Ice. I thank the University of Helsinki, the Arctic Centre, University of Lapland, and the University of Uppsala for facilitating me with all the working resources.

Last and the most important, I would like to thank my father 龚存华 and mother 黄兴兰 for bringing me to this world and putting together all the elements to make this one Doctor of Philosophy.

Contents

List of publications

Paper I: Y. Gong, S. L. Cornford, and A. J. Payne (2014). Modeling the response of Lambert Glacier-Amery Ice shelf system, East Antarctic, to uncertain climate forcing over the 21st and 22nd centuries. The Cryosphere, 8, 1057-1068 (doi: 10.5194/tc-8-1057-2014).

Paper II: R. Gladstone, M. Schäfer, T. Zwinger, Y. Gong, T. Strozzi, J. Moore, R. Mottram, and F. Boberg (2014). Importance of basal processes in simulations of a surging Svalbard outlet glacier. The Cryosphere 8, 1393-1405 (doi: 10.5194/tc-8-1393-2014).

Paper III: Y. Gong, T. Zwinger, S. L. Cornford, R. Gladstone, M. Schäfer and J. Moore (2017). The importance of basal and surface boundary conditions in transient simulations - A case study of a fast-flowing marine terminated glacier in Austfonna, Svalbard. Journal of Glaciology 63 (237), 106-117 (doi:10.1017/jog.2016.121).

Paper IV: Y. Gong, T. Zwinger, J. Åström, B. Altena, T. Schellenberger, R. Gladstone, J. Moore (2017). Simulating the roles of crevasse routing of surface water and basal friction on the surge evolution of Basin 3, Austfonna Ice-cap. The Cryosphere Discuss., in review, (doi: 10.5194/tc-2017-180).

Correspondence: R. Greve, T. Zwinger and Y. Gong (2014). On the pressure dependence of the rate factor in Glen's flow law. Journal of Glaciology, 60 (220), (doi: 10.3189/2014JoG14J019).

Acronyms and Abbreviations

ALOS = Advanced Land Observing Satellite

ASAR = Advanced Synthetic Aperture Radar

a.s.l = above sea level

AWS = Automatic Weather Stations

CSA = Canadian Space Agency

DEM = Digital Elevation Model

DLR = German Aerospace Center

ECHAM5 = European Center/Hamburg model 5

ECMWF = European Centre for Medium-Range Weather Forecasts

ERA = European Reanalysis

ERS = Earth Remote-Sensing Satellite

ESA = European Space Agency

FESOM = Finite Element Sea Ice Ocean Model

GCM = General Circulation Model

GPR = Ground-Penetrating Radar

HadCM3 = Hadley Center coupled model 3

IDW = Inverse Distance Weighting

InSAR = Interferometric Synthetic-Aperture Radar

IPCC AR5 = Intergovernmental Panel on Climate Change 5th assessment report

LG-AIS = Lambert Glacier-Amery Ice Shelf

LMDZ4 = Laboratoire de Météorologie Dynamique Zoom 4

Micro-DICE = Micro-Dynamics of Ice

NCoE SVALI = Nordic Centre of Excellence project 'Stability and Variation of Arctic Land Ice'

NPI = Norwegian Polar Institute

PALSAR = Phased Array type L-band Synthetic Aperture Radar

RACMO = Regional Atmospheric Climate Model

RCM = Regional Climate Model

RES = Radio Echo Sounding

SLE = Sea Level Equivalent

SMB = Surface Mass Balance

TSX = TerraSAR-X

Part I
Overview

1. Introduction

1.1. Motivation

Covering 10% of the global land surface, glacial ice including glaciers, ice caps and ice sheets is the largest reservoir of fresh water on Earth (Vaughan et al., 2013). Glacial ice mass not only modifies local and global climate by altering the energy balance of the lower atmosphere and large scale air circulation (e.g. Broccoli and Manabe, 1987; van den Broeke, 1997; Clark, 1999), but also is one of the most sensitive indicators of climate change and one of the main contributors to sea level change. According to the Intergovernmental Panel on Climate Change 5th assessment report (IPCC AR5; Church et al., 2013; Vaughan et al., 2013), almost all glaciers (i.e., land ice masses excluding the Antarctic and Greenland Ice Sheets) have been shrinking and contribute 0.71 (0.64 to 0.79) mm a^{-1} to sea level rise. The Greenland and Antarctic Ice Sheets have also been losing ice during the last two decades and contributed 0.33 (0.25 to 0.41) mm a^{-1} and 0.27 (0.16 to 0.38) mm a^{-1} respectively to sea level rise between 1993-2010.

The large uncertainty in future projections of sea level contribution due to ice dynamic response to climate change is highlighted in IPCC AR5. The main mechanisms by which climate change can affect the dynamics of ice flow include rapid tidewater glacier retreat, iceberg calving, enhanced basal sliding by surface melt, marine and submarine melt of ice shelves as a consequence of oceanic warming and destabilization of ice shelves by surface water ponding (Church et al., 2013). In order to provide better future projection large scale ice flow models of different complexity are developed to solve these physical problems.

The loss of buttressing from the removal of ice shelves could cause acceleration of grounded outlet glaciers and increase the flux of the inland ice to the ocean (De Angelis and Skvarca, 2003; Rott et al., 2002). One of the challenges of investigating the dynamics of these outlets in the Antarctic Ice Sheet is to properly simulate the region boundary between grounded and floating ice mass, i.e. the grounding line. Also the migration of the grounding line plays an important role in the stability of inland ice masses, especially on retrograde bedrock slopes – the so-called “marine ice sheet instability” (Mercer, 1978). The feedback between the retreat of grounding line to deeper water, floatation, sub-shelf melting, calving, decreased buttressing, increased basal lubrication, ice flow acceleration and grounding line retreat inland requires ice flow models to consider all (at minimum membrane) stresses

across the grounding line and resolve a freely moving grounding line with adequate model resolution (Gladstone et al., 2010; Pattyn et al., 2013).

Representing the fast motion of glacial ice mass is one of the primary aims of ice flow modelling. Most of the fast ice flow is due to motion at the glacial bed, which arises from either sliding over rigid bedrock or bed deformation. The activation of surging glaciers and the recently observed rapid acceleration of marine-terminating glaciers on the Greenland Ice Sheet and the Arctic islands are related to processes at the glacial bed (e.g. Dunse et al., 2015; Gladstone et al., 2014; van de Wal et al., 2008; Zwally et al., 2002). Some of the modern ice flow models assimilate observational surface velocity data to optimize a slip-coefficient distribution obtaining a local linear relationship between basal velocity and driving stress (e.g. MacAyeal, 1993). Other ice flow models use more complex basal velocity - driving stress relations that incorporate basal temperature, effective pressure, till properties etc.(e.g. Hindmarsh, 1997; Iverson et al., 1998; Kamb, 1970, 1991; Lliboutry, 1987). Great effort has also been made to couple ice flow models with basal hydrology models that are capable of simulating sediment property change, basal water pressure evolution and the interaction between them (van de Wel et al., 2013; Werder et al., 2013).

Last but not the least, process based projections of large scale land ice are still hampered by the coupling between ice flow and the climate system. Fully coupled climate and ice dynamic simulations tend to be computational expensive. Alternative methods, such as using downscaled surface mass balance (SMB, Schäfer et al., 2015) or sub-shelf melt rate from climate or ocean model as input at the upper or lower boundary to the ice flow model (Helsen et al., 2012; Sun et al., 2016), have also been developed. When linking climatic signal to abrupt changes of ice dynamics, certain indirect processes such as surface melt routing to the bed should also be taken into account, (Dunse et al., 2015; Zwally et al., 2002).

1.2. Objectives

The present study demonstrates the implementation of ice flow models for future projections of Lambert Glacier-Amery Ice Shelf drainage system, Eastern Antarctica and ice dynamic simulations of a surging glacier in Basin 3, Austfonna Ice-cap. Paper I is a continuation of the author's Master of Research degree project. Paper II and III contribute to the Nordic Centre of Excellence project 'Stability and Variation of Arctic Land Ice' (NCoE SVALI). Paper III also contributes to the European Science Foundation research networking Programme on the Micro-Dynamics of Ice (Micro-DICE). The author is also partly founded by the Väisälä Foundation.

This thesis aims at providing the following general remarks on the application of ice flow models in studying the evolution of glacial ice mass under climate change:

- Off-line coupling the glacier system with the climate system by employing a hierarchy of models from global climate models, through high resolution regional atmospheric and oceanic models, to an ice flow model (Paper I);
- Employing adaptive mesh refinement (Paper I);
- Employing inverse modelling (Paper I, II, III and IV);
- Conducting sensitivity tests with ice flow models (Paper I and III);
- A continuum to discrete multi-model approach (Paper IV).

Specifically, the stability and sea level contribution of Lambert Glacier-Amery Ice Shelf drainage system under climate change over 21st and 22nd centuries and the role of certain topographic features in ice dynamic changes are investigated in Paper I. The dominating factors and potential mechanisms of the surge in Basin 3, Austfonna Ice-cap are studied in Paper II, III and IV. The correspondence discusses the interchangeability of the two expressions of the rate factor in Glen's flow law.

1.3. Structure of the thesis

This thesis is divided into two parts. Part I, of which this introduction constitutes the first chapter, provides an overview of author's studies and a summary of main results and conclusions from the publications. Chapter 2 provides background knowledge about glacier motion and dynamics. Chapter 3 gives an overview of the numerical models. Chapter 4 introduces the study sites LG-AIS drainage system, East Antarctica and Basin 3, Austfonna Ice-cap and the input data for model set-up. Chapter 5 summaries the main results and key findings from the four papers. Chapter 6 closes Part I with conclusions and suggestions for future work.

Part II comprises of four papers and one correspondence listed in the section 'List of publications'.

2. Glacier Motion and Dynamics

This chapter provides an overview of the theoretical basis related to glacier motion and dynamics, upon which the ice dynamic studies of the thesis are built, mainly following the books Cuffey and Paterson (2010) and Benn and Evans (2013) as well as other reference literature cited in the texts.

2.1. Glacier Flow

Glacier flow reflects the response of a glacier to the climate system and is the fundamental process that an ice flow model aims to simulate. Ice mass is transported by glacier flow from high elevation accumulation areas or continental interiors to areas where ice is lost by melting and calving. Ice discharge through any cross-section on a glacier that is in steady state equals the rate of net mass gain upstream. And the departure from steady state (glacier advance or recession) is due to changes in rates of accumulation/ablation, basal sliding or deformational flow due to temperature boundary condition. Glacier flow is driven by gradients in the force exerted by the ice (the driving stress) and resisted by the drag at the glacier boundaries and ice viscosity.

Glaciers can flow by internal deformation and basal motion. In the case of a frozen bedrock, the internal deformation in association with both the vertical and horizontal gradients of the ice flow completely control the flow velocity profile (Fig. 2.1). Internal deformation can generate rapid motion, for instance the upper location along Jakobshavn, where rapid shearing results from large stresses, thick

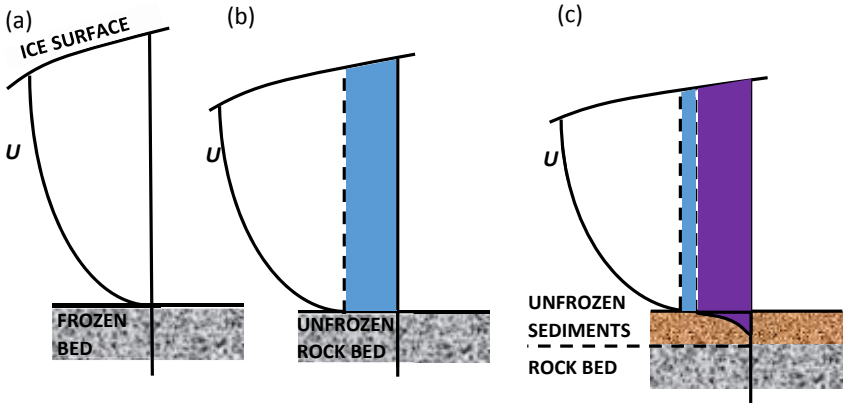

Figure 2.1 Schematic diagram showing the velocity profile (U) from the contribution of (a) Ice deformation only (white); (b) Ice deformation (white) and basal sliding (blue); and (c) Ice deformation (white), basal sliding (blue) and deformation of subglacial sediments (purple). The vertical scale in the sediment bed is exaggerated relative to the ice thickness (Figure is modified from Boulton, 1996).

ice and warm ice at depth (p. 293; Cuffey and Paterson, 2010). In most cases of fast flowing ice masses, such as glacial surges, ice streams etc., the contribution of internal deformation to surface ice flow velocity is exceeded by basal motion.

Deformation of Ice

The deformation of ice under stress consists of ice creep and fracture. The former is the permanent process of glacier motion. The latter plays an important role in processes such as iceberg calving and crevasse formation.

Flow laws that describe the relationship between long-term, steady creep of ice and applied stress have been developed based on numerous laboratory experiments and observations of glacier flow. The most widely used relationship is Glen's flow law (Glen, 1955), which represents the behaviour of ice at secondary creep. Glen's flow law was firstly adapted to glaciers by Nye (1957). The simplest form, describing the relationship between a dominant shear stress τ and the shear strain rate $\dot{\varepsilon}$, follows a power law:

$$\dot{\varepsilon} = A\tau^n , \qquad (2.1)$$

where n is the flow law exponent and A is the rate factor which is affected by temperature, hydrostatic pressure as well as the water content, density, grainsize, impurities and preferred-orientation of ice crystals organized in grains (the fabric of the ice). The dependency of A on pressure and temperature is discussed in the Correspondence included in this thesis. Based on numerous in-situ measurements a value of n=3 is often adopted for glaciological study, which is used for all the simulations in this thesis, suggesting that ice is a strongly non-linear shear thinning material.

Ice fracturing (crevasse opening) happens due to brittle failure when yield stress of ice is exceeded. To model crevasse opening in a continuum model leads to simplification of the effect of the fracturing to certain parameterization such as the depth of the penetration (Cook et al., 2014; Nick et al., 2010, 2013), bulk 'damage'(Borstad et al., 2012), or ice softness (Vieli et al., 2006). On the other hand the discrete element model used in paper IV simulate crevasse formation as microscopic scale discrete process based on first principal fracture physics.

Basal Motion

Glacial basal motion consists of ice sliding over the bed and the deformation of the bed itself. The mechanisms describing ice that slide on rigid beds and deformable beds are referred as hard-bed and soft bed mechanism, respectively. In the latter case, the deformation of a thin layer of the substrates is activated by the sliding of the ice at the ice-substrate interface. In glaciological studies, sliding relations

that describe the relationship between basal velocity, shear stress, basal properties such as water pressure and volume, bed topography and sediment properties are developed based on those mechanisms to analyse glacier flow.

The earliest mechanisms for hard-bed sliding introduced by Weertman (1957) assume that ice is at its pressure melting point and moves past bumps in the bedrock. Weertman's theory of sliding is based on the mechanism of regelation, in which the meltwater produced on the upstream side of the bumps due to pressure contrast flows around the bump and refreeze on the downstream side of the bumps, and enhanced creep, in which increased deformation of ice due to the interaction between ice and bumps allows the ice to move over and around the bump.

Further development of the hard-bed mechanism introduces the role of water-filled and linked cavities emphasizing the importance of water pressure in sliding. Cavities, i.e. ice-bedrock separation, form and enlarge in the lee of the bumps when water pressure at the bed exceeds the minimum value of the compressive normal pressure exerted by the ice on the bed. Sliding rate gets increased because that stresses concentrate on the remaining areas of contact and that basal drag decreased as water pressure increases (e.g. Gagliardini et al., 2007).

Soft-bed sliding fundamentally differs from hard-bed sliding. It requires the presence of at least a thin layer of substrate at the ice-bed interface and involves the sliding of ice along the top of the substrate and the deformation of the substrate at depth. Thus the resistance of the movement of ice at the bed is limited by the strength of the substrates.

Apparently the presence of water at the bed is a key factor in both hard-bed and soft-bed sliding mechanisms. In hard-bed sliding, increased water pressure at the bed due to supplies from geothermal and frictional heating as well as surface meltwater reaching the bedrock decreases effective pressure (i.e., the ice-overburden reduced by the water pressure). It also enlarges cavities thereby reducing the contact area between ice-sheet and substrate. This feedback can result in reduced basal friction and increase in sliding rate. In soft-bed sliding, the feedbacks between water pressure and till deformation can be either positive or negative due to the processes taken place at the ice-till interface such as efficient drainage, frictional heating, dilation and compression. Such feedbacks can be used to explain phenomena of fast ice flow evolution, e.g. glacier surge, which are discussed in paper II and IV.

2.2. Ice Shelves

The first publication included in the thesis examines the dynamics of Amery Ice Shelf in East Antarctica. An ice shelf is the floating portion of an ice sheet, or occasionally a valley glacier. Ice

shelves spread under their own weight. The net outward-directed deviatoric stress arising from gravitational and buoyant forces at the ice front is accommodated by outward creep of the ice. A hypothetical free-floating, unconfined ice shelf does not exert upglacier-directed force as it has no resistance at the lateral margins or at the bedrock. However, most of the ice shelves are grounded at the sides by lateral margins of fjord or islands (confined ice shelves), of which the driving force is balanced by basal friction at the transition area between grounded and floating ice mass and the more dominant lateral friction at the sides. Thus ice flow velocity at the centreline should increase strongly with the width of the shelf (Sanderson, 1979). This applies to the case of the Amery Ice Shelf, Antarctic (Budd et al., 1982).

In the case of confined ice shelves, the back force (per unit width across-shelf), F_B, exerted by the ice shelf and transmitted upstream to the grounded ice consists of side drag from the lateral walls (buttressing), τ_w ,and basal drag, τ_b, on grounded regions of the otherwise floating ice shelf and can be expressed as:

$$F_B = \int_x^{x_m} (\tau_w + \tau_b) dx = \int_x^{x_m} \left(\int_B^S \frac{\partial \tau_{xy}}{\partial y} dz + \tau_b \right) dx, \qquad (2.2)$$

of which the axes and variables can be found in Fig. 2.2. The horizontal shear stress, τ_{xy}, ranges from 50 to 150 kPa; the integration is between the bottom, B, and surface, S, of the ice shelf; x_m is the horizontal distance of the front margin of the ice shelf from the grounding line at $x=0$ and x-axis follows a flow line along the length of the ice shelf.

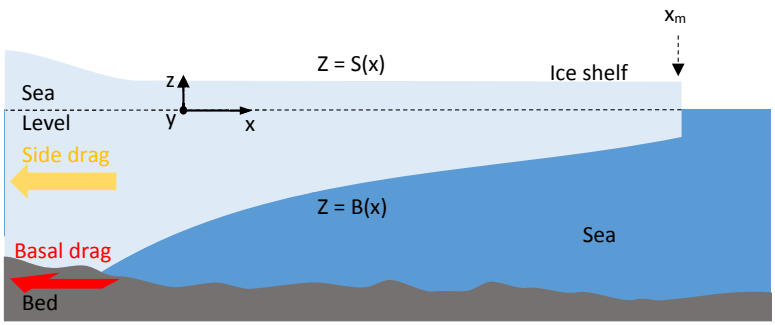

Figure 2.2 Schematic diagram showing coordinates and variables for analysis of the force balance of confined ice shelves (dimension not to scale; Figure is modified from Cuffey and Paterson, 2010, p.374).

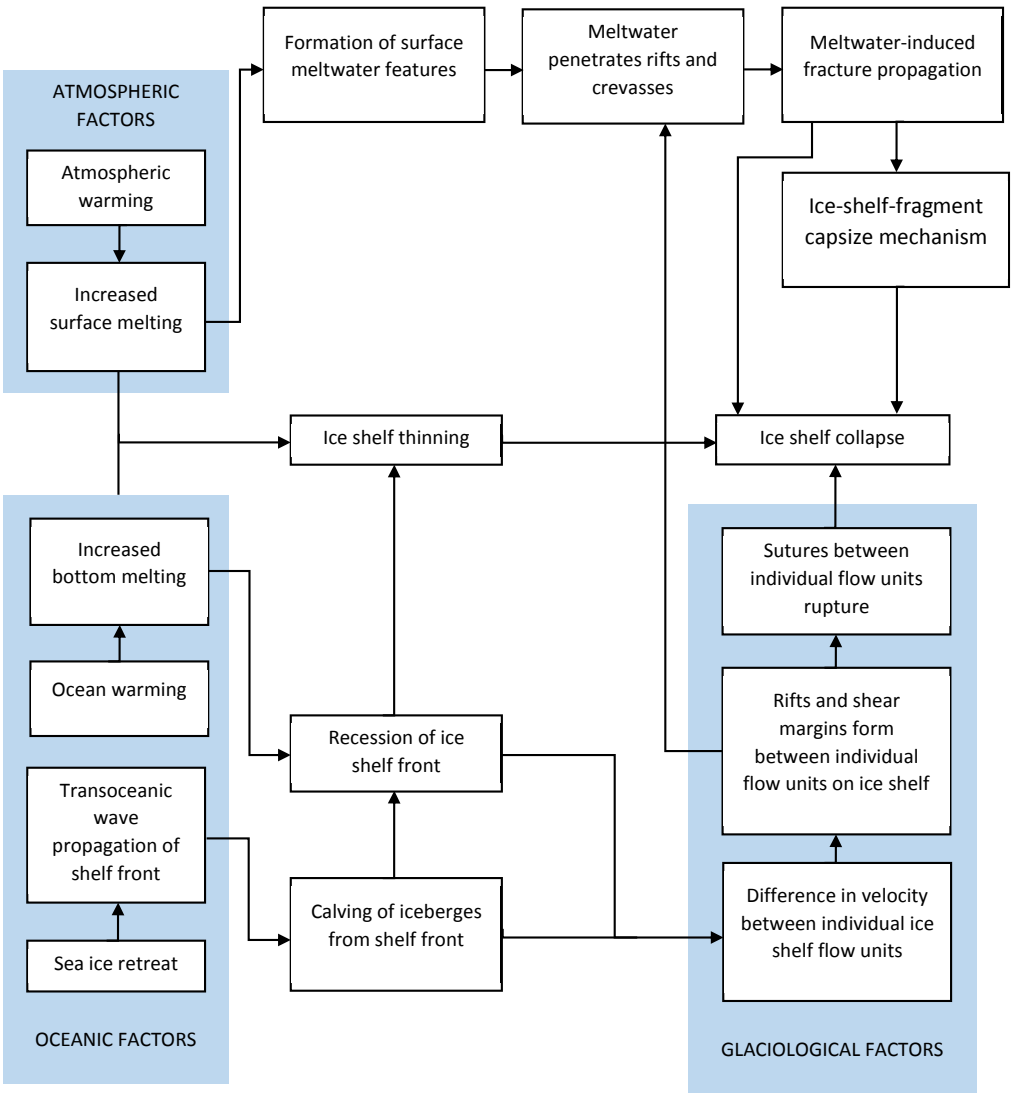

Figure 2.3 Flow chart showing the network of factors controlling ice shelf collapse (figure after Benn and Evans, 2010, p.186).

The variation of back force (F_B) due to the migration of the grounding zone affects the stability of the grounded ice sheets. The grounding zone (also called as grounding line in many literatures) is the boundary between grounded and floating ice mass, i.e. the region over which tidal lifting and dropping

or bedrock irregularities cause partial grounding. The migration of the grounding line may either be an advance in the case of positive mass balance, or more typically under climate warming, retreat. Retreating grounding lines are usually caused by the thinning or removal of the ice shelves as warming oceans thin them via increased sub-shelf melting (Liu et al., 2015). The thinning and disintegration of ice shelves observed in Antarctic Ice Sheet has been related to both atmospheric and oceanic warming (Liu et al., 2015), which has been investigated for Amery Ice Shelf in this thesis. The feedback involved in the mechanism is shown in Fig. 2.3.

Moreover, for feeding glaciers of the ice shelves partly resting on retro-slope bedrock that are below sea level, such as the Lambert Glacier, the retreat of the grounding line, due to atmospheric and oceanic warming, would result in thicker ice grounded in deeper water. This can cause increased flux-gate that would subject the grounded ice sheet to a positive feedback loop that involves floatation, basal melting, increased iceberg production, and further retreat and cause trigger acceleration and thinning of the inland ice sheet (Marine Ice Sheet Instability; Schoof, 2007).

2.3. Glacier Surges

The surging behaviour of the outlet glacier in Basin 3, Austofnna is investigated in Paper II to IV. Surging glaciers are glaciers switching between a long period of slow flowing phase (quiescent phase) and a relatively short period of fast flowing phase (active phase) quasi-periodically. The surge of temperate glaciers are characterized by abrupt acceleration within a few months and sudden termination of the active phase (e.g. Dolgushin et al., 1963; Eisen et al., 2005). Temperate glaciers with partially frozen bed, however, have more gradual build-up period and longer active phase which lasts over decades (Fowler et al., 2001; Frappé and Clark, 2007). Polythermal tidewater glaciers in Svalbard tend to have a relatively long quiescent phase (50-500 years) and a long active phase for over decades (Strozzi et al., 2002). In contrast with the abrupt speed-up in flow velocity of temperate glaciers in Alaska the surge of these glaciers start steadily from the flat lower tongue of the glaciers followed by multi-year acceleration (Luckman et al., 2002; Murray et al., 2003). Then the deceleration happens gradually over years (Murray et al., 2003).

The surge of the polythermal glacier in Basin 3, Austfonna Ice-cap, Svalbard exhibited both long-term steady acceleration and abrupt seasonal summer speed-up events, which is exceptional from other Svalbardic surging glaciers (Dunse et al., 2015; Schellenberger et al., 2017, in review)

In quiescent phase surging glaciers accumulate mass in their reservoir area and build up gravitational driving force through thickening and steepening. The triggering factors of the activation of the surge active phase are often believed to be internal (Meier and Post, 1969; Sharp, 1988). However external factors such as atmospheric warming also play a role by interacting with internal processes via changes in surface mass balance or basal conditions (e.g. Dunse et al., 2015; Gladstone et al., 2014; Meier and Post, 1969).

Hard-bed hydrological switch mechanisms have been discovered for temperate surging glaciers. In general they suggest that the acceleration and deceleration of the ice flow are linked to the change of basal effective pressure caused by the switching of the basal drainage system between an ineffective distributed system developed in winter and an effective conduit system developed in summer (Eisen et al., 2005; Kamb et al., 1985).

Given the fact that most of the temperate surging glaciers lie on deformable bed, existing mechanisms of surge activation also address the importance of the deformation of sub-glacial sediment and the evolution of the sub-glacial hydrology system. Those mechanisms suggest that the initiation of the active phase is due to the deformation of the sediment patches. They get enlarged and connected during the quiescent phase due to the build-up of glacier mass and an initial increase of basal water pressure (p. 533, Cuffey and Paterson, 2010). Then the deformation of the sediment disrupts the effective drainage of the conduit system. This disruption then triggers a feedback involves increased water pressure, reduced sediment strength, enlargement of the slippery deformable patches and other factors (Fig. 2.4).

The same mechanism can be adopted for polythermal glaciers with additional constraints. The slow initiation and termination of the active phase of a slow surge might be related to the lack of water input from en-glacial drainage system at the beginning of the surge and a slowly developing sub-glacial drainage system because of the partially frozen bed. For a completely frozen bed the limiting factor is the evolution of the thermal regime that determines the warming up and refreezing of the bed. Obviously, water supply from the supra- and en-glacial drainage system to the sub-glacial drainage system is crucial for both the initiation and evolution of the surge active phase.

A detailed discussion of the feedback involving melt water input, bed deformation, thermal regime evolution and speed-up of the ice flow during the surge of the polythermal glacier in Basin 3, Austfonna Ice-cap is also presented in paper II and IV.

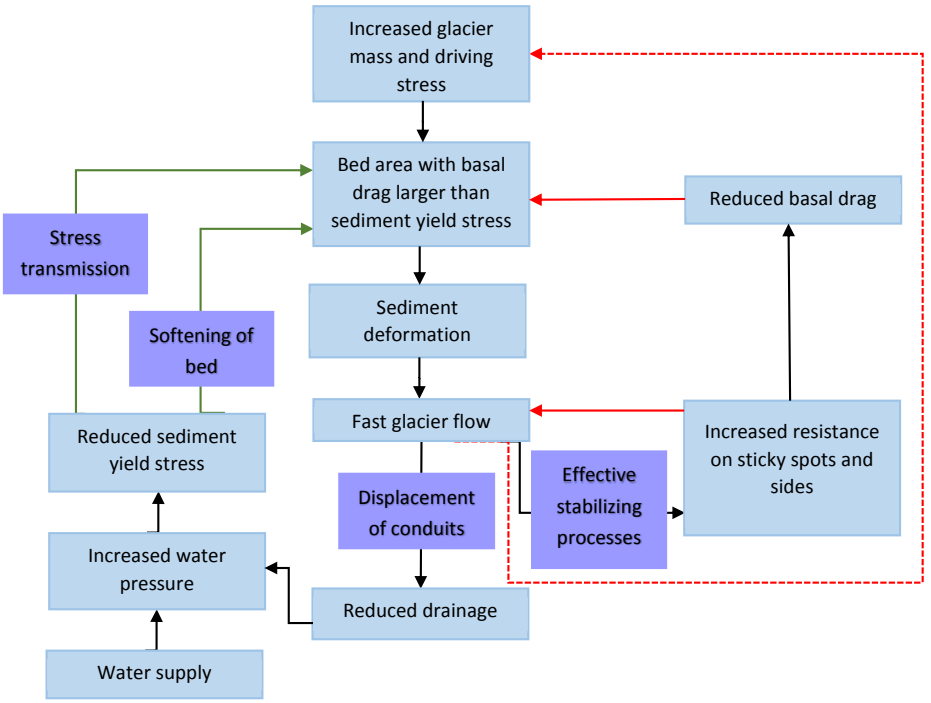

Figure 2.4 Schematic chart of feedback loops in soft bedrock surging mechanism modified from Cuffey and Paterson (p. 532, 2010). Blue boxes are the properties. Purple boxes contain the processes. Black lines lead to the results, red lines indicate a decrease in the target property and green lines indicate an increase. A closed loop of lines with an odd number of red lines indicates a negative feedback, whereas a closed loop with an even number (or zero) of red lines indicates a positive feedback. The dashed line indicates that a surge ends eventually because of depleted glacier mass.

3. Numerical Models

Two ice flow models are used in this thesis. The BISICLES Ice Dynamic model is used to carry out future projections of Lambert Glacier-Amery Ice shelf system in paper I and for sensitivity tests in paper III. The Elmer/Ice Ice Dynamic model is used to carry out simulations for the entire Austfonna Ice-cap in paper II as well as for the glacier in Basin 3, Austfonna Ice-cap in paper III and IV.

Ice flow models are widely used to better understand the behaviour of glaciers and their response to external forcing. They are based on certain fundamental laws or assumptions and are simplified to

allow for an analytical or numerical solution and treat ice as a viscous, incompressible fluid. Diagnostic or prognostic problems are solved based on the conservation laws for mass, linear momentum and internal energy. In glaciology, ice flow can be computed by solving Stokes equations, which express the conservation of linear momentum:

$$\nabla \cdot \boldsymbol{\sigma} + \rho_i \boldsymbol{g} = \nabla \cdot \boldsymbol{\tau} - \nabla \mathrm{p} + \rho_i \boldsymbol{g} = 0, \quad (3.1)$$

and the mass conservation for an incompressible fluid:

$$\nabla \cdot \boldsymbol{u} = \mathrm{tr}(\dot{\boldsymbol{\varepsilon}}) = 0, \qquad (3.2)$$

in which ρ_i is the ice density, $\boldsymbol{g} = (0,0,-g)$ the gravity vector, $\boldsymbol{u} = (u,v,w)$ the ice velocity vector, $\boldsymbol{\sigma} = \boldsymbol{\tau} - p\boldsymbol{I}$ the Cauchy stress tensor with $p = -\mathrm{tr}(\boldsymbol{\sigma})/3$ the isotropic pressure, $\boldsymbol{\tau}$ the deviatoric stress tensor, $\boldsymbol{I}$ the identity matrix and $\dot{\boldsymbol{\varepsilon}}$ the strain-rate tensor.

Equations 3.1 and 3.2 are also called full-Stokes equations since sometimes approximation are made to neglect certain stress components depending on the simplification needed for the force balance of the ice flow.

In addition, a discrete element model, HiDEM (Helsinki Discrete Element Model), is used for solving problems that demands the mechanical description of brittle fracture , such as crevasse formation, iceberg calving, rheological weakening of ice, in which ice is described using discontinues elastic particles. A continuum to discrete multi-model approach between the Discrete Element Model, HiDEM, and Elmer/Ice is used in paper IV to investigate the potential way of linking surface melt through crevasses to basal processes in Basin 3.

An automated mesh refinement technique as a component of BISICLES is implemented in paper I to keep fine mesh resolution at the moving grounding line of Amery Ice shelf. Inverse modelling has been carried out to derive the friction coefficient from the observed surface velocities for the basal sliding relation in paper I, II, III and IV.

Descriptions of the governing equations of the ice flow models, the concept of the fracture formation of the desecrate element model as well as other numerical and data assimilation techniques will be provided in the following sub-sections.

3.1. Elmer/Ice Ice Dynamic Model

Elmer/ice is an add-on package to the open-source, multi-physics Finite Element Model suite Elmer for computational glaciology. Some of the governing equations are presented below. More details can be found in Gagliardini et al. (2013).

The simulations with Elmer/Ice are carried out by considering a gravity-driven flow of incompressible and non-linearly viscous ice flowing over a rigid bed. And the ice flow is computed by solving the unaltered full-Stokes equations (Eq. 3.1 and 3.2).

In this thesis the simulations carried out using Elmer/Ice all assume that ice behaves as an isotropic material. In this case the constitutive relation for ice rheology can be described by Glen's flow law (Glen, 1955):

$$\boldsymbol{\tau} = 2\mu\dot{\boldsymbol{\varepsilon}}, \qquad (3.3)$$

where the effective viscosity μ is defined as

$$\mu = \frac{1}{2}(EA)^{-1/n}\dot{\varepsilon}_e^{(1-n)/n}, \quad (3.4)$$

in which $\dot{\varepsilon}_e^2 = tr(\dot{\boldsymbol{\varepsilon}}^2)/2$ is the square of the second invariant of the strain rate tensor; E is the enhancement factor, which - due to considerations linked to anisotropy - is expected to exceed unity-value for grounded ice of polar ice sheets, whereas taking a value lower than unity if applied to floating ice shelves (Ma et al., 2010); A is the rate factor calculated via Arrhenius law:

$$A = A_0 \exp\left(-\frac{Q + pV}{RT}\right), \qquad (3.5)$$

where A_0 is the pre-exponential constant, Q is the activation energy, p is the pressure, V is the activation volume and $R =$ 8.321 J mol^{-1} K^{-1} is the universal gas constant.

By dropping V and replacing the absolute temperature T by the temperature relative to pressure melting point T' the simplified rate factor can be used:

$$A = A_0 \exp\left(-\frac{Q}{RT'}\right), \qquad (3.6)$$

$$T' = T + \beta p, \qquad (3.7)$$

In the Correspondence to the Journal of Glaciology included in this thesis, we demonstrated that the consistency between Eq. 3.5 and Eq. 3.6 is given due to the fact of a small Clausius-Clapeyron constant β.

The upper surface, $Z_s\ (x, y, z)$, evolves with time through an advection equation:

$$\frac{\partial Z_s}{\partial t} + u_s\frac{\partial (Z_s)}{\partial x} + v_s\frac{\partial (Z_s)}{\partial y} - w_s = M_s, \qquad (3.8)$$

where (u_s, v_s, w_s) is the surface velocity vector obtained from the Stokes solution , M_S is the meteoric accumulation/ablation rate.

For all the simulations carried out with Elmer/Ice in this thesis a linear relation linking basal shear stress, $\boldsymbol{\tau_b}$, to basal velocity, $\boldsymbol{u_b} = (u_b, v_b, w_b)$, is applied:

$$\boldsymbol{\tau_b} = -C\boldsymbol{u_b}. \quad (3.9)$$

The spatial distribution of the basal friction coefficient C is determined by solving an inverse problem, as described in Sect. 3.5.

3.2. BISICLES Ice Dynamic Model

BISICLES is a parallel, adaptive, high-performance ice dynamic model built on the Software for Adaptive Solution of Partial Differential Equations – Chombo (Adams et al., 2015). Some of its governing equations are presented in this section. More detailed description of the model can be found in Cornford et al. (2013)

Instead of solving the unaltered Stokes equations (Eq. 3.1 and 3.2) for the stress-balance equation across the whole model domain, BISICLES employs a depth-integrated hybrid model which is constructed from the higher-order Blatter-Pattyn model and is able to be vertically integrated (Schoof and Hindmarsh, 2010). The Schoof-Hindmarsh model includes longitudinal and lateral stresses and a simplified treatment of vertical shear stress and is more suited to ice shelves and fast-flowing ice streams than areas where vertical deformation is significant.

Ice shelves are assumed to be in local hydrostatic equilibrium, so that the grounding line is determined by a simple flotation criterion, and the upper surface elevation Z_s is related to given bedrock elevation, Z_b, and ice thickness, h, through:

$$Z_s = max\left[h + Z_b, \left(1 - \frac{\rho_i}{\rho_w}\right)h\right], \qquad (3.10)$$

where ρ_i and ρ_w are the densities of ice and sea water.

The ice thickness h and surface horizontal velocity (u_s, v_s) satisfy a two-dimensional mass transport equation:

$$\frac{\partial h}{\partial t} + \frac{\partial (u_s h)}{\partial x} + \frac{\partial (v_s h)}{\partial y} = M_s + M_b, \qquad (3.11)$$

and the two-dimensional stress-balance equation:

$$\nabla \cdot [\phi h \bar{\mu}(2\dot{\boldsymbol{\varepsilon}} + 2tr(\dot{\boldsymbol{\varepsilon}})\boldsymbol{I})] + \boldsymbol{\tau_b} = \rho_i g h \nabla Z_s\,, \qquad (3.12)$$

where M_s and M_b are the meteoric accumulation rate, applied to the upper surface of the entire ice volume, and the oceanic melt rate, applied to the under-side of ice shelves; $\dot{\boldsymbol{\varepsilon}}$ is the horizontal strain-rate tensor

$$\dot{\boldsymbol{\varepsilon}} = \frac{1}{2}[\nabla \boldsymbol{u} + (\nabla \boldsymbol{u})^T], \qquad (3.13)$$

and $\boldsymbol{I}$ is the identity matrix. All vector components and operators in Eq. 3.11 and Eq. 3.12 apply only to the horizontal plain.

The depth-averaged effective viscosity $\phi h\bar{\mu}$ is computed by integrating the vertically varying effective viscosity $\mu(x, y, z)$ between the glacier base (Z_s-h) and the free surface (Z_s):

$$\phi h\bar{\mu}(x,y) = \phi \int_{s-h}^{s} \mu(x,y,z)dz\,, \qquad (3.14)$$

$$2\mu A(4\mu^2\dot{\boldsymbol{\epsilon}}^2 + |\rho_i g(s-z)\nabla Z_s|^2)^{\frac{n-1}{2}} = 1, \qquad (3.15)$$

where $\rho_i\, g(Z_s - z)\nabla Z_s$ is the vertical shear component simplified according to the shallow ice approximation (Cornford et al., 2013), $n = 3$ is Glen's flow law exponent, ϕ is a stiffening factor (or, equivalently, ϕ^{-n} is an enhancement factor), and A depends on the ice temperature T through an empirical equation described by Hooke (1981),

$$A = A_0 \exp[\frac{3f}{(T_r - T)^k} - \frac{Q}{RT}]\,, \qquad (3.16)$$

where $Q = 78.8$ kJ mol^{-1} is the activation energy, $A_0 = 0.093$ Pa^{-3} a^{-1}, $f = 0.53$ K^k, $k = 1.17$ and $T_r = 273.39$ K are empirically determined constants from a wide variety of experiments. Note that since an inverse problem is solved (described in Sect. 3.5) to find the coefficient ϕ, the precise form of A is not crucial.

The basal shear stress, $\boldsymbol{\tau_b}$, is calculated from a linear viscous friction law:

$$\boldsymbol{\tau_b} = \begin{cases} -C\boldsymbol{u_b} & if\ \frac{\rho_i}{\rho_w}h > -b \\ 0 & otherwise \end{cases}, \qquad (3.17)$$

where $\boldsymbol{u_b}$ is the basal velocity vector. Like ϕ, C will be determined by solving an inverse problem, as described in Sect. 3.5.

3.3. HiDEM Discrete Element Model

The discrete element model HiDEM is a first-principle model for fracture formation and dynamics. The purely elastic version, which is sufficient for the purposes of locating fractures if geometric boundary conditions and basal friction coefficient are provided, is used to simulate the facture formation in paper IV. The concept of the fracture formation of the model is introduced in this section. Detailed theoretical description can be found in Åström et al. (2013, 2014).

In HiDEM a large ice-body is divided into discrete particles connected by massless beams. To initialize the simulation, particles are densely packed (close-packed) or randomly deposited to form a large body by assuming that they are frozen together. The frozen contacts between the particles are modelled by elastic massless beams. Fracture takes place if the total stress exceeds a fracture criterion.

3.4. Mesh Construction

Mesh refinement is an optimum practice for large scale simulations with realistic settings in order to achieve low computational costs and small compromises for performance. With certain specific physical problems to solve, such as grounding line migration in the case of LG-AIS system and fast ice flowing area in the case of the surge in Basin 3, spatially varying (and time adaptive, if necessary) mesh is needed to obtain higher resolution only at the area of interest in the model domain.

An unstructured finite element mesh is used for the simulations in Elmer/Ice. The mesh generation starts from a regular mesh of the 2-D footprint confined by the outline of the study area in the mesh generation tool GMSH (Geuzaine and Remacle, 2009). The spatial refinement of the resolution can be carried out by prescribing the desired size of the elements in different parts of the mesh in GMSH or according to the observed surface speed (Fig. 3.1). In the latter case the adjustment is done using the fully automatic, adaptive, isotropic, surface re-meshing procedure YAMS (Frey and Alauzet, 2005).

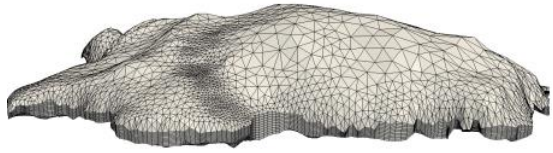

Figure 3.1 An example of the unstructured mesh used for Austfonna Ice-cap model set-up in Elmer/Ice with resolution ranging from 0.25 to 2.5 km refined according to the ice surface speed. The mesh is vertically extruded with 10 equally spaced layers. Vertical exaggeration in this figure is 30 times.

BISICLES discretizes the mass and stress balance equations on block-structured, non-uniform meshes using a finite volume method, supported by the Chombo Adaptive Mesh Refinement framework (Adams et al., 2015). The two-dimensional rectangular meshes are composed of a hierarchy of cell-cantered level domains (Martin et al., 2008) of uniform grids with resolution Δx^{ℓ}, with $0 \leq \ell \leq L$ and $2\Delta x^{\ell+1} = \Delta x^{\ell}$, in which L is the maximum level of the refinement (Fig. 3.2). The refinement can be carried out throughout the simulation to maintain finer resolution along the grounding line region or

fast flowing region. The refinement criteria for determining the location of the refinement is according to flow velocity gradient or grounding line location proximities or both.

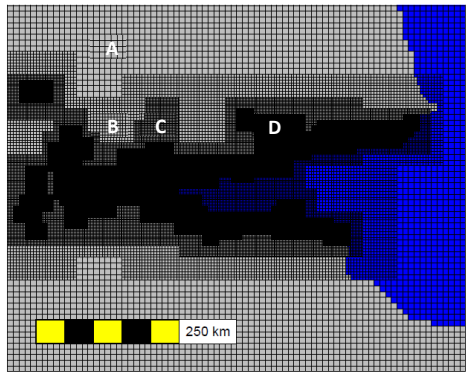

Figure 3.2 Example block structure mesh of Amery Ice Shelf region in BISICLES. Discrete level domain marked with 'A' (ℓ=0) comprises the cell centres of the coarsest grids (Δx=10 km), while the corresponding cell faces make up the two supplementary face-centred level domains. The discrete level domain marked with 'B' (ℓ=1) and the corresponding face-centred level domains are built from all the rectangular blocks that have the resolution Δx=5 km; for discrete level domains marked with 'C' (ℓ=2) and 'D' (ℓ=3), the resolutions of the blocks are Δx=2.5 km and Δx=1.25 km, respectively.

The refined 2-D meshes are then extruded in the vertical with equally spaced layers to form a 3-D structure in both BISICLES and Elmer/Ice.

3.5. Inverse Modelling

Basal friction condition is important in determining the fast ice flow and effected by many complex processes. In ice flow modelling friction parameters are often used in simplified sliding relation to represent those processes. Since their values in-situ are poorly constrained (Gagliardini et al., 2013) inverse modelling is used to obtain those parameters from the largely available remote spatial observations.

In Elmer/Ice two inverse methods are implemented to derive basal friction coefficient C in Eq. 3.9. Both methods are based on minimising a cost function measuring the mismatch between the modelled and observed surface velocity magnitude. The details of the relevant equations can be found in Gillet-Chaulet et al. (2012).

Robin inverse method, detailed in Arthern and Gudmundsson (2010), solves the *Neumann*-type problem defined by the Stokes equations (Eq. 3.1 and 3.2) and stress-free surface boundary condition and the associated *Dirichlet*-type problem defined by the same equations but a Dirichlet condition where observed surface horizontal velocity components are imposed. The cost function of the mismatch between the solutions of the two problems is written as:

$$J_m = \int_{\Gamma_s} (\boldsymbol{u^N} - \boldsymbol{u^D}) \cdot (\boldsymbol{\sigma}^N - \boldsymbol{\sigma}^D) \cdot \boldsymbol{n} d\Gamma, \qquad (3.18)$$

where superscripts *N* and *D* refer to the Neumann and Dirichlet problem solutions, respectively; $\boldsymbol{n}$ is the normal vector.

Control inverse method used in Elmer/Ice is similar to those of MacAyeal (1993) and Morlighem et al. (2010), in which Newton linearization is used so that the Stokes system is independent of the velocity and is self adjoint. The computation of the adjoint of the Stokes system is the key of the method and the cost function expressing the difference between the norm of the modelled and observed horizontal velocities is written as:

$$J_m = \int_{\Gamma_s} \frac{1}{2} (|\boldsymbol{u_H}| - |\boldsymbol{u_H^{obs}}|)^2 d\Gamma, \qquad (3.19)$$

where $\boldsymbol{u^{obs}}$ is the observed velocity vector and subscript *H* refers to horizontal velocity components .
A similar control inverse method (Joughin et al., 2009; MacAyeal, 1993; Morlighem et al., 2010) is also used in BISICLES to derive both basal friction coefficient *C* in Eq. 3.17 and basal stiffening factor φ in Eq. 3.14 in paper I as well as only *C* in paper III. More details of the relevant equations can be found in Cornford et al. (2015).

4. Study Sites and Input Data

This chapter gives an overview of the topographic features, geometry, mass balance and other observations of the two study sites set up in this thesis. Lambert Glacier - Amery Ice shelf system, East Antarctic has been studied in paper I. Basin 3, Austfonna has been studied in paper II, III and IV.

Short descriptions of observational data used in each paper are also summarised in this chapter. They are required for numerical simulations of real-would cases. Topographic data are needed for defining the model domain and hence defining the driving force in the simulation. Surface velocities are needed

for inverse modelling used to determine basal conditions such as friction and basal melt in conjunction with the ice dynamics models. Climate forcing are input as boundary conditions at the upper or lower boundaries that effect the evolution of the ice body when doing prognostic simulations.

4.1. Lambert Glacier - Amery Ice shelf system

Three dimensional forward simulations have been carried out with observational data of Amery Ice Shelf, East Antarctica in Paper I. Amery Ice Shelf is the largest ice shelf in East Antarctica in terms of area (62620 km^2; Scambos et al., 2007) and is at the head of Prydz Bay between the Lars Christensen Coast and Ingrid Christensen Coast (Fig. 4.1). There are eight tributary glacial basins feeding the ice shelf amongst which Fisher, Mellor and Lambert Glacial basin reach the southernmost grounding line and account for 72.15% of the drainage area (Yu et al., 2010). These eight feeding basins and Amery Ice shelf constitute one of the largest glacial systems on the Earth (1380000 km^2). To keep the convention, we refer the system as Lambert Glacier - Amery Ice Shelf drainage system in this thesis. There are few ice free topographic features in the system which play important roles in the stability of the ice dynamics, such as the narrow and deep Lambert Graben through which the ice is drained and Clemence Massif that sticks out from the southern end of the ice shelf.

In general the grounded portion of the system is thought to be in balance or gaining mass (Liu et al., 2015; Sun et al., 2016; Wen et al., 2008; Yu et al., 2010) even though the mass budget of the drainage basins varies widely in different studies due to the difference in the proposed average-accumulation rates for the feeding basins and differences in ice influx calculation across the grounding line. Calving events from Amery Ice Shelf are rare. The iceberg calving flux estimated by Liu et al. (2015) is 0.2±.0 Gt a^{-1} for the period 2005-2011. The ice shelf is also losing mass by sub-shelf melting with net basal mass loss rate ranging from less than 10 to around 103 Gt a^{-1} in different modelling and observational studies (Depooter et al., 2013; Galton-Fenzi et al., 2012; Liu et al., 2015).

Although Amery Ice Shelf has long been considered a stable ice shelf the future state of the whole drainage system has large uncertainties under the influence of the global warming. Thus through the future projections over the 21st and 22nd centuries, ice dynamic changes, global sea level contribution, the differing roles of accumulation and sub-shelf melting as well as the influence of topographic features on the dynamics of the system have been investigated in the study.

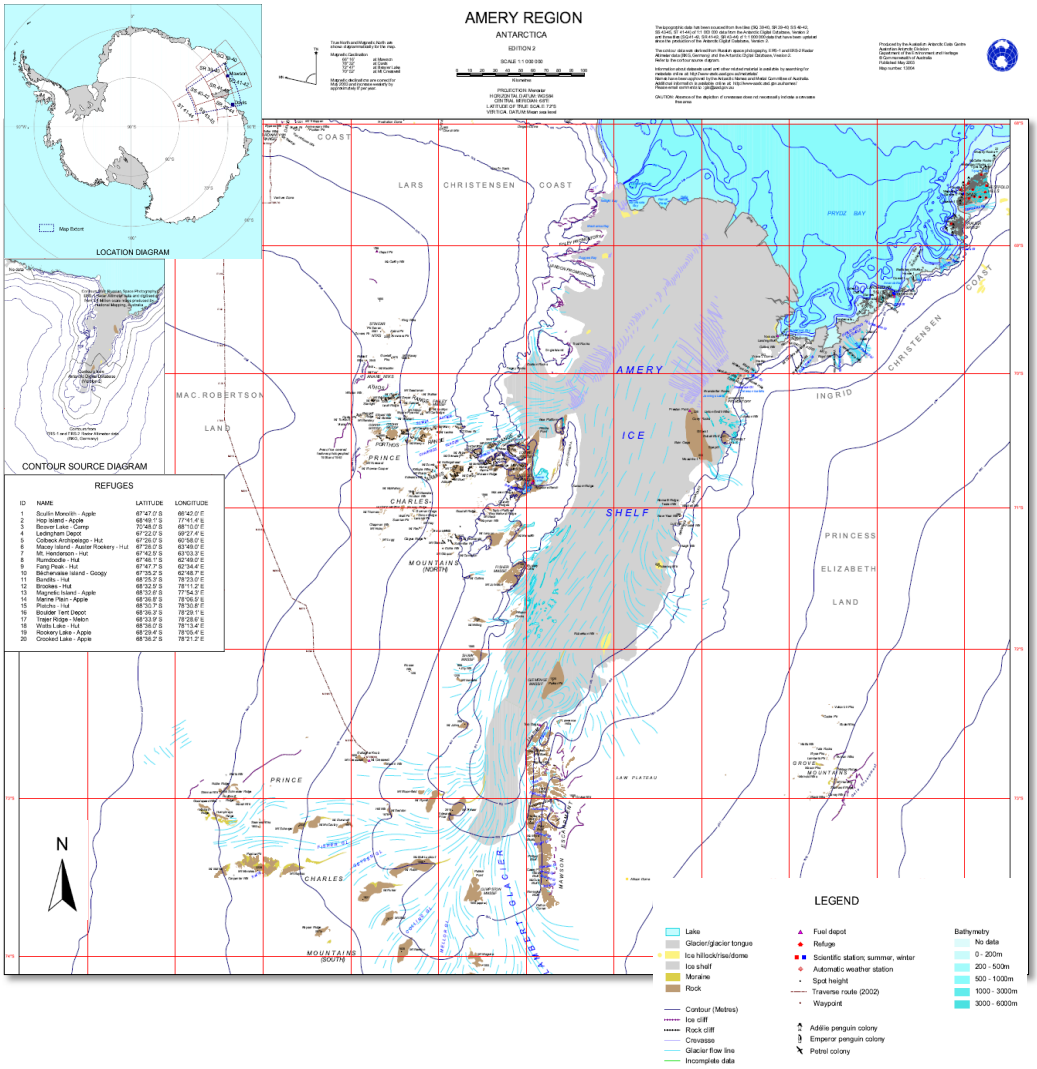

Figure 4.1 Map of the Amery Ice Shelf, its locations on the Antarctic Ice Sheet and its feeding glaciers (produced by the Australian Antarctic Data Center; © Commonwealth of Australia). The topographic data has been sourced from five files (SQ 39-40, SR 39-40, SS 40-42, SS 43-45, ST 41-44) of 1:100 0000 data from the Antarctic Digital Database, Version 2 and three tiles (SQ 41-42, SR 41-42, SR 43-44) of 1:100 0000 data that have been updated since the production of the Antarctic Digital Database, Version 2. The contour data was derived from Russian space photography, ERS-1 and ERS-2 Radar Altimeter data (BKG, Germany) and the Antarctic Digital Database, Version 2.

Topography Observations

The topographic data for setting up the simulations includes ice thickness and bedrock topography data drawn from the 5 km ALBMAP Digital Elevation Model (DEM; Le Brocq et al., 2010). The basic mask for the whole Antarctic delineating ocean, grounded ice sheet, ice shelf region and the initial grounding line area is obtained from the Mosaic of Antarctic coastline shape files (Scambos et al., 2007). Modifications have been made to the grounding line in order to smoothly combine the grounded ice sheet, which is largely from BEDMAP data sets (Lythe et al., 2001), with the ice shelf. The basal topography and marine bathymetry is based on the BEDMAP data sets supplemented by data from ALBMAP. The ice thickness data of grounded ice is produced by incorporating the original BEDMAP ice thickness with the AGASEA/BBAS data for West Antarctic (Holt et al., 2006; Vaughan et al., 2006). The ice shelf thickness is derived by hydrostatic assumption from surface elevations.

Surface Velocity Observations

The surface velocity data taken from multiple satellites Interferometric Synthetic-Aperture Radar (InSAR) acquired during the years 2007 to 2009 (Rignot et al., 2011) is used for basal friction coefficient inversion.

The complete InSAR measurements consist of spring 2009 data from RADARSAT-2 (Canadian Space Agency (CSA) and MacDonald, Dettwiler, and Associates Limited); spring 2007, 2008, and 2009 data from Envisat Advanced Synthetic Aperture Radar (ASAR; European Space Agency (ESA)]; and fall 2007 to 2008 data from the Advanced Land Observing Satellite (ALOS) Phased Array type L-band Synthetic Aperture Radar (PALSAR; Japan Aerospace Exploration Agency), complemented by patches of CSA's RADARSAT-1 data from fall 2000 (Jezek et al., 2003) and ESA's Earth Remote-Sensing Satellites 1 and 2 (ERS-1/2) data from spring 1996 (Rignot et al., 2008). The data are georeferenced with a precision better than 300 m to an Earth-fixed grid by using a DEM of Bamber and Gomez-Dans (2005) and calibrated with control points in coast-to-coast ASAR tracks.

Climate Forcing

The surface mass balance and sub-shelf melt rate underneath the ice shelf from a hierarchy of climate models are used to drive the future projections.

Two greenhouse gas emission scenarios, A1B and E1, are used to force the General Circulation Models (GCMs) in order to simulate the 21th century (2000-2099) and 22nd century (2000-2199) condition. Then data from GCMs, including Hadley Center coupled model 3 (HadCM3; Pope et al., 2000) and the European Center/Hamburg model 5 (ECHAM5; Marsland et al., 2003; Roeckner et al., 2003), are used to provide boundary forcing for the Regional Climate Model (RCMs). RCMs have higher resolution

and allow more detailed process studies and simulation of regional condition by dynamical downscaling. The RCMs employed include Regional Atmospheric Climate MOdel (RACMO2; van Meijgaard et al., 2008), Laboratoire de Météorologie Dynamique Zoom 4 (LMDZ4; Hourdin et al., 2006) and Finite Element Sea Ice Ocean Model (FESOM; Wang et al., 2014).

4.2. Austfonna Ice-cap and Basin 3

Three dimensional simulations with different numerical models with observational data sets from different time period are carried out in Paper II, III and IV to investigate the surging behaviour of the out-let glacier in Basin 3, Austfonna Ice-cap, Svalbard.

Austfonna (~8000 km^2) is the7th largest ice-cap on Earth and constitutes the largest individual ice body on the Svalbard archipelago in the high arctic. It is located on eastern Nordauslandet (Fig. 4.2).

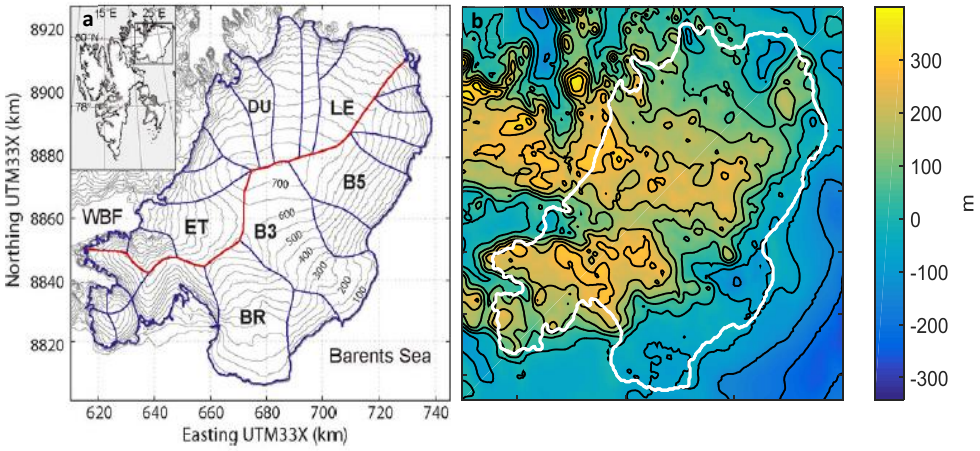

Figure 4.2 (a) A map of Austfonna ice cap and its location within the Svalbard archipelago (insert). Contours spaced at 50 m show surface elevations (m a.s.l). The red solid line indicates the main ice divide. The main basins outlined with blue solid lines and marked with bold letters are: the three known surge-type basins, Basin 3 (B3) and Bråsvellbreen (BR), terminating into the Barents Sea, Etonbreen (ET), terminating into Wahlenbergfjorden (WBF); as well as other basins, Duvebreen (DU), Leighbreen (LE) and Basin-5 (B5). (b) The bedrock topography and marine bathymetry. The white solid line in indicates the observed glacier outline. ((a) is from Dunse et al., 2011).

Austfonna rises to about 800 m above sea level at its main summit and consists of two types of drainage basins which are separated by a southwest-northeast oriented ice divide (Dowdeswell et al., 1986; Moholdt and Kääb, 2012). The northwestern basins contain mostly land-terminating glaciers or

glaciers that terminate in narrow fjords; southeastern basins are mainly filled with marine-terminating glaciers that are grounded on bedrock below sea level at their termini and calve icebergs to northern Barents Sea.

The ice cap has a distinct southeast to northwest accumulation gradient as the main moisture source is the Barents Sea located in the southeast. The interior of the ice cap has been thickening since at least 1986 while the overall volume change in the 2002-2008 period is negative (-0.16 ± 0.06 m w.e. a^{-1}) due to the retreat of the calving front (Moholdt et al., 2010; Taurisano et al., 2007). The sea-level rise contribution during the same period, which is before the dramatic acceleration of the outlet in Basin 3 starting from 2010, is considered to be close to zero (Moholdt et al., 2010).

There are three known surge-type basins on Austfonna (Fig. 4.2a): Etonbreen (1938 or earlier), Bråsvellbreen (1937–38) and Basin 3 (between 1850 and 1873). The surging glacier in Basin 3 has entered its active phase again recently. Therefore our study is focused on investigating the ice dynamic changes of the glacier in Basin 3.

Basin 3 (Fig. 4.2a), with its poly-thermal outlet glacier, is located in southeastern Austfonna and is grounded as much as 150 m below sea level at its terminus (Dowdeswell et al., 1986; Dunse et al., 2011). Although there is no direct observation of the lithology of the bedrock, sediment-laden meltwater outflow (Pfirman and Solheim, 1989) and submarine sediment ridges (Solheim and Pfirman, 1985) have been observed in front of Basin 3, indicating that the marine grounded areas are to some extent underlain by sediments and subjected to basal water flow (Dowdeswell et al., 1999; Macheret and Vasilenko, 1988). The northern flow unit of the outlet is constrained by a sub-glacial trough which consists of an over-deepening area in the lower part of the glacier (Fig. 4.2b).

The step-wise multi-annual acceleration of the northern flow unit began in the early 1990s super-imposed with short-lived abrupt speed-up events after each summer melt season observed since 2008. In autumn 2012 the former slow-flowing southern unit became activated after the unplugging of the frozen bed at the ice front. Then the two fast-flow units merged and reached the maximum (20 m d^{-1}) velocity in January 2013 (Dunse et al., 2015). The sea-level rise contribution of Basin 3 is 7.2 ±2.6 Gt a^{-1} during the peak of the surge (April 2012 to May 2013; Dunse et al., 2015).

The step-wise multi-annual acceleration of the northern flow since 1995 is believed to be related to sub-glacial hydrology system and till deformation. The seasonal speed-up events observed since 2008 is likely to link to summer melt induced ‘hydro-thermodynamic’ feedback (Dunse et al., 2015). Thus

the coupling between the ice dynamic model and the sub-glacial hydrology model as well as the representation of processes for routing surface meltwater down to the glacier bed are need to capture the evolution of the surge in Basin 3. All these research theories are investigated and discussed in the studies of the three publications with multiple numerical models and up-to-date observational data.

Topography Observations

The surface and bedrock topography data from Dunse et al. (2011) are used for the simulations in paper II and III.

The DEM providing the surface elevation above sea level at 250m resolution is based on the Norwegian Polar Institute (NPI) 1: 250 000 topographic maps derived from aerial photography and airborne Radio Echo Sounding (RES) measurements over Austfonna in 1983. The marine bathymetry (2 km horizontal resolution) is from the International Bathymetry Chart of the Arctic Ocean, Version 2.0 (Jakobsson et al., 2008).The ice thickness used for generating bedrock elevation is based on airborne RES data published by Dowdeswell et al. (1986) and is supplemented with two data sets from 2008 (Vasilenko et al., 2009).The surface elevation and ice thickness data used are then all resampled onto a 1.0×1.0 km grid mesh (Dunse et al., 2011). Bedrock elevation was derived by pointwise subtracting the ice thickness value from the surface elevation.

The simulations in paper IV use the same bedrock DEM but different surface elevation data. The surface elevation data is derived from Cryosat altimetry data acquired during July 2010 – December 2012 (McMillan et al., 2014). The measurements acquired over a succession of orbit cycles that are within 2-5 km^2 geographic regions are grouped together for the final product.

Surface Velocity Observations

The horizontal surface velocities acquired by satellite remote sensing measurements in 1995, 2008 and 2011 are used for basal friction coefficient inversion in paper II. The same velocity fields in 1995 and 2011 are also used for mesh refinement. The 1995 surface velocity field is calculated using InSAR from the Tandem Phase ERS-1/2 SAR observation obtained between December 1995 and January 1996 (Dowdeswell et al., 2008). The 2008 surface velocity field is calculated using offset tracking (Pohjola et al., 2011) from four ALOS PALSAR scenes acquired between January 2008 and March 2008 with a 46-day time interval. The 2011 surface velocity field is calculated with a combined InSAR and tracking approach from ERS-2 SAR observations obtained between March and April 2011.

The same horizontal surface velocities acquired in 1995 and 2011 are also used for basal friction coefficient inversion in paper III.

In paper IV twenty seven velocity time series maps generated from TerraSAR-X (TSX) satellite SAR scenes (April 2012 – July 2014) (Schellenberger et al., 2017, in review) are used as the input surface velocity data for basal friction coefficient inversion. The original 2m resolution TSX scenes were provided by the German Aerospace Center (DLR) covering only the lower part of Basin 3.
Then the TSX data are stitched on top of two background velocity fields with larger coverage according to the acquiring time. The TSX data derived during 19 April 2012 – 28 December 2012 is stitched with 2011 surface velocity snapshot described above; The TSX data derived after 28 December 2012 is stitched with velocity snapshot from Landsat-8 imagery acquired in April 2013.

Climate Forcing
The SMB from the regional climate model HIRHAM5 (Christensen et al., 2007) is input at the upper boundary as climatic forcing. HIRHAM5 is based on Undén et al. (2002) and ECHAM5 models (Roeckner et al., 2003). It was forced with the European Centre for Medium-Range Weather Forecasts (ECMWF) European Reanalysis (ERA) Interim data set in the atmosphere and sea surface temperature and sea ice concentration also from the ECMWF for the period 1989–2011 (Langen et al., 2014). The physics of the model have been supplemented with a surface snow scheme and SMB calculation for glaciers (Rae et al., 2012). SMB is calculated using the energy balance approach to determine melt rates and a parameterization for retention of liquid water in the snowpack.
The 1990s mean SMB from HIRHAM5 is used in paper II. Bilinear interpolation is used to interpolate from the approximately 5.5 km resolution of HIRHAM5 to the finer-resolution ice flow model mesh.
A downscaling method using SMB-elevation gradients is employed in paper III for the monthly HIRHAM5 SMB time series January 1995 to December 2011.

5. Results

Key results from the future projections of LG-AIS system (paper I) and the investigation of the surge in Basin 3, Austfonna Ice-cap (paper II to IV) are summarized below.

5.1. Future projections of the LG-AIS system

The simulations of future projections over the 21st and 22nd century approximate coupling between LG-AIS and the climate system. Also, by employing extreme forcing, melt rates of 1000 m a^{-1}, over a portion of the ice shelf, effectively removing that part of the shelf entirely within a few years, the degree to which the Amery Ice Shelf buttresses the glaciers at the southern edge is investigated.

Evolution of the ice flow dynamics of LG-AIS system is determined by the melt-rate data. As none of the forcing scenarios applied within the simulations exhibits significant grounding line retreat, it is the

broader pattern of Amery Ice Shelf thinning that drives the changes in grounding line migration and the volume above floatation rather than the melt rates immediately downstream of the grounding line.

In the extreme forcing experiments, the southern grounding line retreats and mass loss significantly increases only when the ice shelf is removed to the area south of Clemence Massif.

The variation between the simulations forced with different climate forcing combinations is dominated by contributions from the SMB input. And the contribution from the LG-AIS system to sea level rise is no more than 3 mm over 220 years driven by the largest sub-shelf melt rate and is confined to 11 mm by removing the ice shelf entirely.

5.2. Surge in Basin 3, Austfonna Ice-cap

The evolution of the basal friction in Basin 3 is assessed through inverse modelling of basal friction coefficients by minimizing the mismatch between the modelled and observed surface velocity magnitude at different time instances from 1995 to 2014 in Elmer/Ice. The simulated surface velocities show a good match to observations. The results show that the basal friction alone was insufficient to balance the driving stress at the early stage of the multi-annual acceleration in 1995. A low friction area had already developed in the central and southern basin in 2011 but was disconnected from the inland region and also behind a stagnant terminus. After August 2012 the stagnant frontal region shrank to a small band at the ice front and the low friction area in the southern basin expanded further inland and connected with the northern low friction area. In January 2013 the low friction area expanded across the entire basin bed with a few particularly deep minima in the south. After January 2013 the basal friction pattern remained almost stable.

Steady-state and transient temperature simulations were carried out with Elmer/Ice to investigate the sensitivity of basal temperature to geothermal heat flux, advection and frictional heat generation at the bed. Frictional heating cannot compensate for adjective heat loss in the steady-state simulation with inverted friction coefficient in 1995. On the contrary, frictional heating causes the basal temperate at pressure melting point under much of the Basin 3 outlet glacier in the steady-state simulation with inverted friction coefficient in 2011.

Transient simulations of 100 years under present-day forcing with friction coefficients of 1995 or 2011 demonstrate that using a temporally fixed basal friction field obtained through inversion can lead to thickness change errors of the order of 2 m a^{-1}.

Transient simulations from January 1995 to December 2011 with basal friction coefficients interpolated temporally between those dates are forced by time varying SMB downscaled from the RCM HIRHAM5 using different strategies. It turns out that the downscaling methodology of SMB have no significant influence on the results for the timescales of our study. A transient simulation of the same time period is also carried out using BISICLES applying the same configuration as in Elmer/Ice to investigate the sensitivity of the results to model physics. No significant differences in the modelled results are found. The dynamic response of the fast flowing area in Basin 3 during that period is governed by the temporal evolution of basal friction coefficient. Ice volume changes and sea-level rise contribution also depend most strongly on the evolution of the basal friction coefficient.

In addition, the simulations aimed to reproduce the dramatic speed-up in the southern part of Basin 3 from January 2012 to June 2013 are carried out by using linearly temporally extrapolated basal friction coefficients or by selectively altering the spatial distribution of basal friction coefficients over different regions of the bed. The results show that a simple continuation of the 1995 to 2011 basal friction trend and spatial pattern cannot reproduce the sudden acceleration of southern Basin 3.

The basal friction coefficient distributions obtained for August 2012 and August 2013 are further used as a boundary condition in a discrete element model HiDEM to generate crevasses distribution. The crevasses distributions at both dates reflect the basal friction patterns and indicates the governing role of basal friction on crevasse formation. The validation between the modelled crevasses distribution and the satellite observation obtained in 4 August 2013 are carried out using the Kappa method (Wang et al., 2016). The Kappa coefficient calculated from the resampled (4.6 × 4.6 km smoothing window) modelled and observed crevasse map suggests substantial agreement (K = 0.71). Although a ~60 degree mismatch of the crevasse orientation appear in the middle upper basin and less dense modelled crevasse distribution in frontal region.

Basal melt water is calculated from an estimated geothermal heat flux, strain heating and basal friction-heating. Relatively high basal melt rates (> 0.005 m a-1), which is mainly caused by frictional heating and still much less than the volumes available from surface melt, appeared at the side walls of the sub-glacial valley around the over-deepening area.

For the configuration at August 2012 we identify crevasses that can potentially penetrate the full length of the glacier and hence act as possible routes for surface water to reach the bedrock. Based on these inlets we then calculate the flow path of basal water at the bed according to hydraulic potential of both surface and basal meltwater.

Hydraulic potential drives the basal water in the northern fast-flow region (sourced from both surface meltwater entering the bed and basal meltwater generated locally) either directly to the terminus or to the sub-glacial over-deepening area, where it potentially can accumulate. Basal water at the southern part of the basin is routed directly towards the terminus of the southern corner of the glacier.

6. Conclusions

Main conclusions of each publication are summarized below. The general remarks and suggestions for future works are also provided in the end.

6.1. Summary of the papers

6.1.1. Paper I

Future projection over the 21st and 22nd centuries of the Lambert Glacier–Amery Ice Shelf system, East Antarctica has been carried out by either employing a hierarchy of models from global IPCC-class climate models, through high resolution regional models of the polar ocean and atmosphere, to the ice flow model BISICELS, or forcing BISICLES with extreme melt rate.

The results of all the simulations suggest that LG-AIS will be rather stable in the face of future atmospheric and oceanic warming. The sea level rise contribution of LG-AIS system is no more than 3mm over 220 years for all the climatic force driven simulations. The Lambert, Fisher and Mellor glaciers are most sensitive to thinning of the ice shelf south of Clemence Massif.

Author's contribution: Pre-processed the input data for the model simulations. Designed and conducted the numerical simulations with the help of the second co-author. Conducted the data analysis and initiated the writing of the paper as well as the preparation of figures. The second co-author later did extra experiments and modification of the texts for the paper revision.

6.1.2. Paper II

Sensitivity experiments consisting of transient simulations under present-day forcing have been carried out with Elmer/Ice, to demonstrate the importance of basal processes for the surge of the outlet glacier in Basin 3, Austfonna Ice-cap, Svalbard. The results suggest that a system of processes and feedbacks involving till deformation and basal hydrology could explain both the seasonal accelerations and the ongoing inter-annual speed-up. The increase in advection of heat due to sliding is likely to limit the duration of the surge phase of Basin 3. A further finding of the article is that subglacial hydrology, including residence times and water routing, and its impact on bed yield strength should be included in model studies aiming to reproduce the surge evolution.

Author's contribution: Conducted model prognostic simulations for the first author. Participated in data analysis and commented on the drafts of the paper.

6.1.3. Paper III

The importance of basal boundary conditions is assessed for transient simulations of Basin 3, Austfonna Ice-cap between January 1995 and December 2011 and for the acceleration starting in 2012, in which basal friction coefficients are inverted from observed surface velocity and temporally interpolated using different scenarios. Time-varying surface mass-balance data from the regional climate model HIRHAM5 are downscaled according to elevation and used as climatic driving force. The sensitivity of results to model choice is also investigated by using two ice flow models, Elmer/Ice and BISICLES. Our model investigations suggest that changes in basal friction patterns, and in turn basal processes are the most important factors for the 2012 acceleration in Basin 3. A soft-bed mechanism that involves the basal hydrology system and till deformation should be included in the future model development. In addition, the representation of processes for routing surface meltwater down to the glacier bed in ice flow models would improve our ability to evaluate the impact of surface boundary condition changes (climate forcing) on model results.

Author's contribution: Designed the numerical experiments together with the co-authors. Pre-processed the input data, conducted the numerical simulations, and analysed the model outputs. Prepared the paper and figures, which were commented on by the co-authors. Co-authors also provided the observational data.

6.1.4. Paper IV

A detailed time series of basal friction coefficients inverted from observed surface velocity data between April 2012 and July 2014 in the continuum ice flow model Elmer/Ice, and crevasse distribution simulated by the discrete element model, HiDEM are used to look at the mechanisms that facilitated the onset and spread of the surge in Basin 3, Austfonna Ice-cap.

The modelled crevasse distribution reflects to a high degree the basal friction coefficient distribution. The flow path calculated according to hydraulic potential of both surface and basal melt water supports the 'hydro-thermodynamic' feedback to summer melt proposed by Dunse et al. (2015). The results indicate either a direct enhancement to the ice flow through basal lubrication or a lagged-in-time mechanism through the outflow of accumulated water in the over-deepening area to explain seasonal speed-up in Basin 3 and the initiation of the acceleration of the southern flow unit in 2012.

Author's contribution: Designed the numerical experiments together with the co-authors. Pre-processed the input data, conducted the numerical simulations with the continuum model, and analysed the model outputs. Prepared the paper and designed the figures, which were commented on by the co-authors. Co-authors also provided the observational data. The third co-author conducted the simulation with discrete element model using the data prepared by the first author.

6.1.5. Correspondence

In Glaciological literature, two significantly different expressions for the rate factor in Glen's flow are communicated. One expressing it in terms of pressure, absolute temperature, activation energy and activation volume (a measurable quantity), the other (used in Elmer/Ice) reducing the factor to include the temperature relative to pressure melting point and activation energy. The paper – for the first time in literature - shows that due to a small value of the Clausius-Clapeyron constant, in a reasonably acceptable approximation these two formulations are equal to each other. This is proved by a positive consistency between measured and (by the latter method) computed activation volumes. Within the range of the certainly large uncertainties imposed by measurements this renders the usually applied simplification of dropping the activation volume to be valid.

Author's contribution: Pointed out the existing (and not previously discussed in the published literature) ambiguity on the expression of the pressure dependence of the rate factor of Glen's flow law. Discussed with the co-authors and commented on the texts of the correspondence.

6.2. General remarks and Outlook

The present studies through ice flow modelling aim to provide better understanding of mechanisms involved in realistic pphysical processes and future projections of ice dynamics. Several general remarks and topics for potential future work will be suggested in this section.

A fixed calving criterion is adopted in all the simulations in this thesis assuming that the calving front was always grounded with a positive height above floatation. For fast flowing outlets like the one in Basin 3, Austfonna, a fixed calving front position can affect the ice dynamics further inland due to the bias in longitudinal stress gradient calculation. In reality the calving front, especially the northern calving front, advanced quite significantly after 2011 (Dunse et al., 2015). Additionally the grounding/floating condition of the ice front in southern Basin 3 could also be an important factor determining the dramatic acceleration in 2012. Although no direct in-situ evidence could be provided to prove that the ice front was partially ungrounded, the calculation from several satellite images suggest that parts of the terminus might have been near floatation prior to 2012 (McMillan et al., 2014).

More efforts can be put on adapting more feasible or physically based calving criteria in future model development to capture the features concerning ice dynamics in frontal region.

As suggested in all the papers concerning the surge in Basin 3, Austfonna (paper II, III and IV) a soft-bed mechanism based hydrology model needs to be added to the ice flow model in order to capture the mutli-annual and seasonal speed up events. However, there are at least three challenges that make this task non-trivial.

First of all, locating the water source is crucial. Several unpublished experiments of coupling the ice flow model Elmer/Ice with a hydrology model (Gong et al., 2014) suggest that the evolution of the basal hydrology system thus the timing and location of the switching are determined by the location of the water source in one drainage event (in one steady-state simulation). In paper IV the authors located those crevasses deep enough to assume that water will penetrate from the surface down to the bedrock, identifying them as a route of surface melt water down to the bed. However eh-glacial drainage system is ignored in the investigation.

Secondly, cryo-hydrological warming (Phillips et al., 2010) obviously plays an important role in the feedbacks discussed in paper II and IV and has not been taken into account in the simulations in this thesis or the other model study on Austfonna done previously (Dunse et al., 2011). By prescribing the location of the water at the bed to calculate the latent heat release from refreezing then to estimate further basal melt water production in a steady state simulation is trivial. However, to interact with the hydrology model is not an easy task.

Lastly, one other important ingredient of coupling ice dynamics with the basal hydrology is a proper basal sliding relation that incorporates effective pressure. In previous unpublished experiments (Gong et al., 2014) the author has used a Coulomb type friction relation (Gagliardini et al., 2007; Schoof, 2005) which describes a non-linear, water pressure dependent relationship between basal shear stress and basal velocities.

One obvious step after solving the problems of representing physical processes more feasibly in numerical models would be to improve future projections. For century scale projections, climatic forcing should still primarily be the determining factor in terms of mass balance and sea level contribution calculation. One-way coupling has been applied to the LG-AIS system (paper I). Two-way offline coupling, i.e. exchanging output between ice flow model and regional climate model, can be applied not only to the LG-AIS but also to other major drainage basins around the Antarctic Ice Sheet. Similar studies have at least been done for the Greenland Ice Sheet (Yang et al., 2014). As discussed in

paper III, further downscaling of SMB from the regional climate model can be crucial in connection with increasing mesh resolution used by ice flow models. For future projection of fast flowing outlets, like the one in Basin 3 that exhibits accelerating behaviour related to summer melt, in particular the input of melt water production from climate models is needed.

References

Adams, M., Colella, P., Graves, D., Johnson, J., Johansen, H., Keen, N., Ligocki, T., Martin, D., McCorquodale, P., Modiano, D., Schwartz, P., Sternberg, T. and van Straalen, B.: Chombo software package for AMR applications – design document, [online] Available from: http://seesar.lbl.gov/anag/chombo/ChomboDesign-3.1.pdf, 2015.

Arthern, R. and Gudmundsson, H.: Initialization of ice-sheet forecasts viewed as an inverse Robin problem, J. Glaciol., 56, 527–533, doi:10.3189/002214310792447699, 2010.

Åström, J., Timo, R., Tallinen, T., Zwinger, T., Benn, D., Moore, J. and Timonen, J.: A particle based simulation model for glacier dynamics, The Cryosphere, 7, 1591–1602, doi:10.5194/tc-7-1591-2013, 2013.

Bamber, J. and Gomez-Dans, J. L.: The accuracy of digital elevation models of the Antarctic continent, Earth Planet. Sci. Lett., 237(3–4), 516–523, doi:10.1016/j.epsl.2005.06.008, 2005.

Benn, D. and Evans, D.: Glacier-climate interactions. In: Glaciers & Glaciation, 2nd ed., Routledge, Oxon, UK and New York, USA., 2010.

Benn, D. and Evans, D.: Glaciers and Glaciation, second., Routledge, Oxon, UK and New York, USA., 2013.

Borstad, C., Khazendar, A., Larour, E., Morlighem, M., Rignot, E., Schodlok, M. and Seroussi, H.: A damage mechanics assessment of the Larsen B ice shelf prior to collapse: Toward a physically-based calving law, Geophys. Res. Lett., 39(18), doi:10.1029/2012GL053317, 2012.

Broccoli, A. and Manabe, S.: The influence of continental ice, atmospheric CO2, and land albedo on the climate of the last glacial maximum, Clim. Dyn., 1(2), 87–99, doi:10.1007/BF01054478, 1987.

van den Broeke, M.: Momentum, Heat, and Moisture Budgets of the Katabatic Wind Layer over a Midlatitude Glacier in Summer, J. Appl. Meteorol., 36, 763–774, doi:10.1175/1520-0450(1997)036<0763:MHAMBO>2.0.CO;2, 1997.

Budd, W., Corry, M. and Jacka, T.: Results from the Amery Ice Shelf Project, Ann. Glaciol., 3, 36–41, doi:10.1017/S0260305500002494, 1982.

Christensen, O. B., Drews, M. and Christensen, J. H.: The HIRHAM Regional Climate Model Version 5 (beta), Technical Report, Danish Meteorological Institute. [online] Available from: http://www.dmi.dk/dmi/tr06-17, 2007.

Church, J., Clark, P., Cazenave, A., Gregory, J., Jevrejeva, S., Levermann, A., Merrifield, M., Milne, G., Nerem, S., Nunn, P., Payne, A., Pfeffer, T., Stammer, D. and Unnikrishnan, A.: Sea Level Change. In: Climate Change 2013: The Physical Science Basis. Contribution of Working Group I to the Fifth Assessment Report of the Intergovernmental Panel on Climate Change, Cambridge University Press, Cambridge, United Kingdom and New York, NY, USA., 2013.

Clark, C.: Glaciodynamic context of subglacial bedform generation and preservation, Ann. Glaciol., 28, 23–32, doi:10.3189/172756499781821832, 1999.

Cook, S., Rutt, I., Murray, T., Luckman, A., Zwinger, T., Sel, N., Goldsack, A. and James, T.: Modelling environmental influences on calving at Helheim Glacier in eastern Greenland, The Cryosphere, 8, 827–841, doi:10.5194/tc-8-827-2014, 2014.

Cornford, S., Martin, D., Graves, D., Ranken, G., Le Brocq, A., Gladstone, R., Payne, A., Ng, E. and Lipscomb, W.: Adaptive mesh, finite volume modeling of marine ice sheets, J. Comput. Phys., 232(1), 529–549, doi:10.1016/j.jcp.2012.08.037, 2013.

Cornford, S., Martin, D., Payne, A., Ng, E., Le Brocq, A., Gladstone, R., Edwards, T., Shannon, S., Agosta, C., van den Broeke, M., Hellmer, H., Krinner, G., Ligtenberg, S., Timmermann, R. and Vaughan, D.: Century-scale simulations of the response of the West Antarctic Ice Sheet to a warming climate, The Cryosphere, 9, 1579–1600, doi:10.5194/tc-9-1579-2015, 2015.

Cuffey, K. and Paterson, S.: The physics of the glaciers, fourth., Butterworth-Heinemann, Burlington, USA and Oxfrod, UK., 2010.

De Angelis, H. and Skvarca, P.: Glacier surge after ice shelf collapse, Science, 299(5612), 1560–1562, doi:10.1126/science.1077987, 2003.

Depooter, M., Bamber, J., Griggs, J., Lenaerts, J., Ligtenberg, S., van den Broeke, M. and Moholdt, G.: Calving fluxes and basal melt rates of Antarctic ice shelves, Nature, 502, 89–92, doi:10.1038/nature12567, 2013.

Dolgushin, L. ., Yevteyev, S. ., Krenke, A. ., Rototayev, K. . and Svatkov, N. .: The recent advance of the Medvezhiy Glacier, Prir. 1963, 11, 85–92, 1963.

Dowdeswell, J., Drewry, D. J., Cooper, A., Gorman, M., Liestol, O. and Orheim, O.: Digital mapping of the Nordaustlandet ice caps from airborne geophysical investigation, Ann. Glaciol., 8, 51–58, 1986.

Dowdeswell, J., Unwin, B., Nuttall, A. M. and Wingham, D.: Velocity structure, flow instability and mass flux on a large Arctic ice cap from satellite radar interferometry, Earth Planet. Sci. Lett., 167(3–4), 131–140, doi:10.1016/S0012-821X(99)00034-5, 1999.

Dowdeswell, J., Benham, T., Strozzi, T. and Hagen, J. O.: Iceberg calving flux and mass balance of the Austfonna ice cap onNordaustlandet, Svalbard, J. Geophys. Res., 113, doi:10.1029/2007JF000905, 2008.

Dunse, T., Greve, R., Schuler, T. V. and Hagen, J. O.: Permanent fast flow versus cyclic surge behaviour:numerical simulations of the Austfonna ice cap, Svalbard, J. Glaciol., 57, doi:10.3189/002214311796405979, 2011.

Dunse, T., Schellenberger, T., Hagen, J. O., Kääb, A., Schuler, T. V. and Reijmer, C.: Glacier-surge mechanisms promoted by a hydro-thermodynamic feedback to summer melt, The Cryosphere, 9, 197–215, doi:10.5194/tc-9-197-2015, 2015.

Eisen, O., Harrison, W., Raymond, C., Echelmeyer, K., Bender, G. and Gorda, J.: Variegated Glacier, Alaska, USA: A century of surges, J. Glaciol., 51(174), 399–406, doi:10.3189/172756505781829250, 2005.

Fowler, A., Murray, T. and Ng, F.: Thermally controlled glacier surging, J. Glaciol., 47, 527–538, 2001.

Frappé, T.-P. and Clark, G.: Slow surge of Trapridge Glacier, Yukon Territory, Canada, J. Geophys. Res. Earth Surf., 112(F3), doi:10.1029/2006JF000607, 2007.

Frey, P. and Alauzet, F.: Anisotropic mesh adaptation for CFD computations, Comput. Methods Appl. Mech. Eng., 194(48–49), 5068–5082, doi:10.1016/j.cma.2004.11.025, 2005.

Gagliardini, O., Cohen, D., Råback, P. and Zwinger, T.: Finite-element modeling of subglacial cavities and related friction law, J. Geophys. Res., 112, doi:10.1029/2006JF000576, 2007.

Gagliardini, O., Zwinger, T., Gillet-Chaulet, F., Durand, G., Favier, L., de Fleurian, B., Greve, R., Malinen, M., Martín, C., Råback, P., Ruokolainen, J., Sacchettini, M., Schäfer, M., Seddik, H. and Thies, J.: Capabilities and performance of Elmer/Ice, a new-generation ice sheet model, Geosci. Model Dev., 6, 1299–1318, doi:10.5194/gmd-6-1299-2013, 2013.

Galton-Fenzi, B., Hunter, J., Coleman, R., Marsland, S. and Warner, R.: Modeling the basal melting and marine ice accretion of the Amery Ice Shelf, J. Geophys. Res., 117(C9), doi:10.1029/2012JC008214, 2012.

Geuzaine, C. and Remacle, J.-F.: Gmsh: a three-dimensional finite element mesh generator with built-in pre- and post-processing facilities, Int. J. Numer. Methods Eng., 79(11), 1309–1331, doi:10.1002/nme.2579, 2009.

Gillet-Chaulet, F., Gagliardini, O., Seddik, H., Nodet, M., Durand, G., Ritz, C., Zwinger, T., Greve, R. and Vaughan, D.: Greenland ice sheet contribution to sea-level rise froma new-generation ice-sheet model, The Cryosphere, 6(6), 1561–1575, doi:10.5194/tc-6-1561-2012, 2012.

Gladstone, R., Lee, V., Vieli, A. and Payne, A.: Grounding line migration in an adaptive mesh ice sheet model, J. Geophys. Res. Earth Surf., 115(F4), doi:10.1029/2009JF001615, 2010.

Gladstone, R., Schäfer, M., Zwinger, T., Gong, Y., Strozzi, T., Mottram, R., Boberg, F. and Moore, J.: Importance of basal processes in simulations of a surging Svalbard outlet glacier, The Cryosphere, 8, 1393–1405, doi:10.5194/tc-8-1393-2014, 2014.

Glen, J.: The Creep of Polycrystalline Ice, Proc. R. Soc., 228(1175), 519–538, doi:10.1098/rspa.1955.0066, 1955.

Gong, Y., Zwinger, T., Gladstone, R., de Fleurian, B., Schäfer, M. and Moore, J.: Implementation of a hydrology model for Basin 3, Austfonna Ice Cap, Svalbard, 2014.

Helsen, M., van de Wal, R., van den Broeke, M., van de Berg, W. J. and Oerlemans, J.: Coupling of climate models and ice sheet models by surface massbalance gradients: application to the Greenland Ice Sheet, The Cryosphere, 6, 255–272, doi:10.5194/tc-6-255-2012, 2012.

Hindmarsh, R.: Deforming beds: viscous and plastic scales of deformation, Quat. Sci. Rev., 16(9), 1039–1056, doi:10.1016/S0277-3791(97)00035-8, 1997.

Holt, J., Blankenship, D., Morse, D., Young, D., Peters, M., Kempf, S., Richter, T., Vaughan, D. and Corr, H.: New boundary conditions for the West Antarctic Ice Sheet: Subglacial topography of the Thwaites and Smith glacier catchments, Geophys. Res. Lett., 33(L09502), doi:10.1029/2005GL025561, 2006.

Hooke, R.: Flow law for polycrystalline ice in glaciers: Comparison of theoretical predictions, laboratory data, and field measurements, Rev. Geophys., 19(4), 664–672, doi:10.1029/RG019i004p00664, 1981.

Hourdin, F., Musat, I., Bony, S., Braconnot, P., Codron, F., Dufresne, J.-L., Fairhead, L., Filiberti, M.-A., Friedlingstein, P., Grandpeix, J.-Y., Krinner, G., LeVan, P., Li, Z. and Lott, F.: The LMDZ4 general circulation model: climate performance and sensitivity to parametrized physics with emphasis on tropical convection, Clim. Dyn., 27, 787–813, doi:10.1007/s00382-006-0158-0, 2006.

Iverson, N., Hooyer, T. and Baker, R.: Ring-shear studies of till deformation: Coulomb plastic behaviour and distributed strain in glacier beds, J. Glaciol., 44, 634–642, doi:10.1017/S0022143000002136, 1998.

Jakobsson, M., Macnab, R., Mayer, L., Anderson, R., Edwards, M., Hatzky, J., Schenke, H. W. and Johnson, P.: An improved bathymetric portrayal of the Arctic Ocean: Implications for ocean modeling and geological, geophysical and oceanographic analyses, Geophys. Res. Lett., 35, doi:10.1029/2008GL033520, 2008.

Jezek, K., Farness, K., Carande, R., Wu, X. and Labelle-Hamer, N.: RADARSAT 1 synthetic aperture radar observations of Antarctica: Modified Antarctic Mapping Mission, 2000, Radio Sci., 38(4), doi:10.1029/2002RS002643, 2003.

Joughin, I., Tulaczyk, S., Bamber, J., Blankenship, D., Holt, J., Scambos, T. and Vaughan, D.: Basal conditions for Pine Island and Thwaites Glaciers, West Antarctica, determined using satellite and airborne data, J. Glaciol., 55(190), 245–257, 2009.

Kamb, B.: Sliding motion of glaciers: theory and observation, Rev. Geophys., 8(4), 673–728, doi:10.1029/RG008i004p00673, 1970.

Kamb, B.: Rheological nonlinearity and flow instability in the deforming bed mechanism of ice stream motion, J. Geophys. Res., 96, 16585–16595, doi:10.1029/91JB00946, 1991.

Kamb, B., Raymond, C., Harrison, W., Engelhardt, H., Echelmeyer, K., Humphrey, N., Brugman, M. and Pfeffer, T.: Glacier Surge Mechanism: 1982-1983 Surge of Variegated Glacier, Alaska, Science, 227(4686), 469–479, doi:10.1126/science.227.4686.469, 1985.

Langen, P., Mottram, R., Christensen, J., Boberg, F., Rodehacke, C., Stendel, M., van As, D., Ahlstrøm, A., Mortensen, J., Rysgaard, S., Petersen, D., Svendsen, K., Aðalgeirsdóttir, G. and Cappelen, J.: Estimating and understanding recent changes in the energy and freshwater budget for Godthåbsfjord catchment with a 5 km regional climate model, Prep., 2014.

Le Brocq, A., Payne, A. and Vieli, A.: An improved Antarctic dataset for high resolution numerical ice sheet models (ALBMAP v1), Earth Syst. Sci. Data, 2, 247–260, doi:5194/essd-2-247-2010, 2010.

Liu, Y., John, M., Cheng, X., Gladstone, R., Bassis, J., Liu, H., Wen, J. and Hui, F.: Ocean-driven thinning enhances iceberg calving and retreat of Antarctic ice shelves, Proc. Natl. Acad. Sci., 112(11), 3263–3268, doi:10.1073/pnas.1415137112, 2015.

Lliboutry, L.: Realistic, yet simple bottom boundary conditions for glaciers and ice sheets, J. Geophys. Res. Solid Earth, 92(B9), 9101–9109, doi:10.1029/JB092iB09p09101, 1987.

Luckman, A., Murray, T. and Strozzi, T.: Surface flow evolution throughout a surge measured by satellite radar interferometry, Geophys. Res. Lett., 29, doi:10.1029/2001GL014570, 2002.

Lythe, M., Vaughan, D. and the BEDMAP Consortium: A new ice thickness and subglacial topographic model of Antarctica, J. Geophys. Res., 106(B6), 11335–11351, doi:10.1029/2000JB900449, 2001.

Ma, Y., Gagliardini, O., Ritz, C., Gillet-Chaulet, F., Durand, G. and Montagnat, M.: Enhancement factors for grounded ice and ice shelves inferred from an anisotropic ice-flow model, J. Glaciol., 56, 805–812, doi:10.3189/002214310794457209, 2010.

MacAyeal, D.: A tutorial on the use of control methods in ice sheet modeling, J. Glaciol., 39, 91–98, 1993.

Macheret, Y. and Vasilenko, E.: Pecularities of internal structure and regime of glaciers on Nordaustlandet by airborne radio-echo sounding data (In Russian with English summary), Data Glaciol. Stud., 62, 44–56, 1988.

Marsland, S., Haak, H., Jungclaus, J., Latif, M. and Röske, F.: The Max-Planck-Institute global ocean/sea ice model with orthogonal curvilinear coordinates, Ocean Model., 5(2), 91–127, 2003.

Martin, D., Colella, P. and Graves, D.: A cell-centered adaptive projection method for the incompressible Navier–Stokes equations in three dimensions, J. Comput. Phys., 227(3), 1863–1886, doi:10.1016/j.jcp.2007.09.032, 2008.

McMillan, M., Shepherd, A., Gourmelen, N., Dehecq, A., Leeson, A., Ridout, A., Flament, T., Hogg, A., Gilbert, L., Benham, T., Michiel van den Broeke, Julian Dowdeswell, Xavier Fettweis, Brice Noël and Tazio Strozzi: Rapid dynamic activation of a marine-basedArctic ice cap, Geophys. Res. Lett., 41, 8902–8909, doi:10.1002/2014GL062255, 2014.

Meier, M. and Post, A.: What are glacier surges?, Can. J. Earth Sci., 6(4), 807–817, doi:10.1139/e69-081, 1969.

van Meijgaard, E., van Ulft, B., van de Berg, W. J., Bosveld, F., van den Hurk, B., Lenderink, G. and Siebesma, P.: The KNMI regional atmospheric climate model RACMO, version 2.1, Technical Report, Royal Netherlands Meteorological Institute, De Bilt., 2008.

Mercer, J.: West Antarctic ice sheet and CO2 greenhouse effect: a threat of disaster, Nature, 271, 321–325, doi:10.1038/271321a0, 1978.

Moholdt, G. and Kääb, A.: A new DEM of the Austfonna ice capby combining differential SAR interferometry with ICESat laseraltimetry, Polar Res., 31, doi:10.3402/polar.v31i0.18460, 2012.

Moholdt, G., Hagen, J. O., Eiken, T. and Schuler, T. V.: Geometric changes and mass balance of the Austfonna ice cap,Svalbard, The Cryosphere, 4, 21–34, doi:10.5194/tc-4-21-2010, 2010.

Morlighem, M., Rignot, E., Seroussi, H., Larour, E., Ben Dhia, H. and Aubry, D.: Spatial patterns of basal drag inferred using control methods from a full-Stokes and simpler models for Pine Island Glacier, West Antarctica, Geophys. Res. Lett., 37, doi:10.1029/2010GL043853, 2010.

Murray, T., Strozzi, T., Luckman, A., Jiskoot, H. and Christakos, P.: Is there a single surge mechanism? Contrasts in dynamics betweenglacier surges in Svalbard and other regions, J. Geophys. Res., 108(B5), 2237, doi:10.1029/2002JB001906, 2003.

Nick, F., van de Veen, C. J., Vieli, A. and Benn, D.: A physically based calving model applied to marine outlet glaciers and implications for the glacier dynamics, J. Glaciol., 56, 781–794, doi:10.3189/002214310794457344, 2010.

Nick, F., Vieli, A., Andersen, M., Joughin, I., Payne, A., Edwards, T., Pattyn, F. and van de Wal, R.: Future sea-level rise from Greenland's main outlet glaciers in a warming climate, Nature, 497, 235–238, doi:10.1038/nature12068, 2013.

Nye, J.: The Distribution of Stress and Velocity in Glaciers and Ice-Sheets, Proc. R. Soc., 239(1216), 113–133, doi:10.1098/rspa.1957.0026, 1957.

Pattyn, F., Perichon, L., Durand, G., Favier, L., Gagliardini, O., Hindmarsh, R., Zwinger, T., Albrecht, T., Cornford, S., Docquier, D., Fürst, J., Goldberg, D., Gudmundsson, H., Humbert, A., Hütten, M., Huybrechts, P., Jouvet, G., Kleiner, T., Larour, E., Martin, D., Morlighem, M., Payne, A., Pollard, D., Rückamp, M., Rybak, O., Seroussi, H., Thoma, M. and Wilkens, N.: Grounding-line migration in plan-view marine ice-sheet models: results of the ice2sea MISMIP3d intercomparison, J. Glaciol., 59, 410–422, doi:10.3189/2013JoG12J129, 2013.

Pfirman, S. and Solheim, A.: Subglacial meltwater discharge in the open-marine tidewater glacier environment: observations from Nordaustlandet, Svalbard Archipelago, Mar. Geol., 86(4), 265–281, 1989.

Phillips, T., Rajaram, H. and Steffen, K.: Cryo-hydrologic warming: A potential mechanism for rapid thermal response of ice sheets, Geophys. Res. Lett., 37, doi:10.1029/2010GL044397, 2010.

Pohjola, V., Christoffersen, P., Kolondra, L., Moore, J., Pettersson, R., Schäfer, M., Strozzi, T. and Reijmer, C.: Spatial distribution and change in the surface ice-velocity field of Vestfonna ice cap, Nordaustlandet, Svalbard, 1995–2010 usinggeodetic and satellite interferometry data, Geogr. Ann. Ser. Phys. Geogr., 93, 323–335, doi:10.1111/j.1468-0459.2011.00441.x, 2011.

Pope, V., Gallani, M., Rowntree, P. and Stratton, R.: The impact of new physical parametrizations in the Hadley Centre climate model: HadAM3, Clim. Dyn., 16(2–3), 123–146, doi:10.1007/s003820050009, 2000.

Rae, J., Aðalgeirsdóttir, G., Edwards, T., Fettweis, X., Gregory, J., Hewitt, H., Lowe, J., Lucas-Picher, P., Mottram, R., Payne, A., Ridley, J., Shannon, S., van de Berg, W., van de Wal, R. and van de Broeke, M.: Greenland ice sheet surface mass balance: evaluating simulations and making projections with regional climate models, The Cryosphere, 6, 1275–1294, doi:10.5194/tc-6-1275-2012, 2012.

Rignot, E., Bamber, J., van den Broeke, M., Davis, C., Li, Y., van de Berg, W. J. and van Meijgaard, E.: Recent Antarctic ice mass loss from radar interferometry and regional climate modelling, Nat. Geosci., 1, 106–110, doi:10.1038/ngeo102, 2008.

Rignot, E., Mouginot, J. and sch, B.: Ice Flow of the Antarctic Ice Sheet, Science, 333(6048), 1427–1430, doi:10.1126/science.1208336, 2011.

Roeckner, E., Bäuml, G., Bonaventura, L., Brokopf, R., Esch, M., Giorgetta, M., Schlese, U., Schulzweida, U., Kirchner, I., Manzini, E., Rhodin, A. and Tompkins, A.: The atmospheric general circulation model ECHAM 5. Part I: Model description, Max-Planck-Institut für Meteorologie, Hamburg, Germany., 2003.

Rott, H., Rack, W., Skvarca, P. and De Angelis, H.: Northen Larsen Ice Shelf, Antarctica: further retreat after collapse., Ann. Glaciol., 34, 277–282, doi:10.3189/172756402781817716, 2002.

Sanderson, T.: Equilibrium profile of ice shelves, J. Glaciol., 22, 435–460, 1979.

Scambos, T., Haran, T., Fahnestock, M., Painter, T. and Bohlander, J.: MODIS-based Mosaic of Antarctica (MOA) data sets: Continent-wide surface morphology and snow grain size, Remote Sens. Environ., 111(2–3), 242–257, doi:10.1016/j.rse.2006.12.020, 2007.

Schäfer, M., Möller, M., Zwinger, T. and Moore, J.: Dynamic modelling of future glacier changes: mass balance/elevation feedback in projections for the Vestfonna ice cap, Nordaustlandet, Svalbard, J. Glaciol., 61, 1121–1136, doi:10.3189/2015JoG14J184, 2015.

Schellenberger, T., Dunse, T., Kääb, A., Schuler, T. V., Hagen, J. O. and Reijmer, C.: Multi-year surface velocities and sea-level rise contribution of the Basin-3 and Basin-2 surges, Austfonna, Svalbard, Cryosphere Discuss, doi:10.5194/tc-2017-5, 2017.

Schoof, C.: The effect of cavitation on glacier sliding, Proceeding R. Soc. A, 461, 609–627, doi:10.1098/rspa.2004.1350, 2005.

Schoof, C.: Ice sheet grounding line dynamics: steady states, stability and hysteresis, J. Geophys. Res. Earth Surf., 112, doi:10.1029/2006JF000664, 2007.

Schoof, C. and Hindmarsh, R.: Thin-Film Flows with Wall Slip: An Asymptotic Analysis of Higher Order Glacier Flow Models, Q. J. Mech. Appl. Math., 63, 73–114, doi:10.1093/qjmam/hbp025, 2010.

Sharp, M.: Surging glaciers: behaviour and mechanisms, Prog. Phys. Geogr., 12(3), 349–370, 1988.

Solheim, A. and Pfirman, S.: Sea-floor morphology outside a grounded, surging glacier - Bråsvellbreen,Svalbard, Mar. Geol., 65(1–2), 127–143, 1985.

Sun, S., Cornford, S., Gwyther, D., Gladstone, R., Galton-Fenzi, B., Zhao, L. and Moore, J.: Impact of ocean forcing on the Aurora Basin in the 21st and 22nd centuries, Ann. Glaciol., 57(73), 1–8, doi:10.1017/aog.2016.27, 2016.

Taurisano, A., Schuler, T. V., Hagen, J. O., Eiken, T., Loe, E., Melvold, K. and kohler, J.: The distribution of snow accumulation across the Austfonna ice cap, Svalbard: direct measurements and modelling, Polar Res., 26, 7–13, doi:10.1111/j.1751-8369.2007.00004.x, 2007.

Undén, P., Rontu, L., Järvinen, H., Lynch, P., Calvo, J., Cats, G., Cuxart, J., Eerola, K., Fortelius, C., Garcia-Moya, J., Jones, C., Lenderink, G., McDonald, A., McGrath, R., Navascues, B., Nielsen, N., _degaard, V., Rodriguez, E., Rummukainen, M., Room, R., Sattler, K., Sass, B., Savijärvi, H., Schreur, B., Sigg, R., The, H. and Tijm, A.: HIRLAM-5 Scientific Documentation, [online] Available from: http://hirlam.org, 2002.

Vasilenko, E., Navarro, F., Dunse, T., Eiken, T. and Hagen, J. O.: New low-frequency radio-echo soundings of Austfonna Ice Cap, Svalbard, in The Dynamics and Mass Budget of Arctic Glaciers. Extended abstracts, Canada., 2009.

Vaughan, D., Corr, H., Ferraccioli, F., Frearson, N., O'Hare, A., Mach, D., Holt, J., Blankenship, D., Morse, D. and Young, D.: New boundary conditions for the West Antarctic ice sheet: subglacial topography beneath Pine Island Glacier, Geophys. Res. Lett., 33(L09501), doi:10.1029/2005GL025588, 2006.

Vaughan, D., Comiso, J., Allison, I., Carrasco, J., Kaser, G., Kwok, R., Mote, P., Murray, T., Paul, F., Ren, J., Rignot, E., Solomina, O., Steffen, K. and Zhang, T.: Observations: Cryosphere. In: Climate Change 2013: The Physical Science Basis. Contribution of Working Group I to the Fifth Assessment Report of the Intergovernmental Panel on Climate Change, Cambridge University Press, Cambridge, United Kingdom and New York, NY, USA., 2013.

Vieli, A., Payne, A., Du, Z. and Shepherd, A.: Numerical modelling and data assimilation of the Larsen B ice shelf, Antarctic Peninsula, Philos. Trans. R. Soc. Math. Phys. Eng. Sci., 15, 1815–1839, doi:10.1098/rsta.2006.1800, 2006.

van de Wal, R., Boot, W., van den Broeke, M., Smeets, P., Reijmer, C., Donker, J. and Oerlemans, J.: Large and Rapid Melt-InducedVelocity Changes in the AblationZone of the Greenland Ice Sheet, Science, 321(5885), 111–113, doi:10.1126/science.1158540, 2008.

Wang, enli, Annette, R., John, M., Xuefeng, C., Duoying, J., Q, L., N, Z., Chenghai, W., Shiqiang, Z., David, L., Dave, U. G. S., Wenxin, Z., Christine, D., Charles, K., Kazuyuki, S., Andrew, M., Eleanor, B. and B, D.: Diagnostic and model dependent uncertainty of simulated Tibetan permafrost area, The Cryosphere, 10, 287–306, doi:10.5194/tc-10-287-2016, 2016.

Wang, Q., Danilov, S., Sidorenko, D., Timmermann, R., Wekerle, C., Wang, X., Jung, T. and Schröter, J.: The Finite Element Sea Ice-Ocean Model (FESOM) v.1.4: Formulation of an ocean general circulation model, Geosci. Model Dev., 7, 663–693, doi:10.5194/gmd-7-663-2014, 2014.

Weertman, J.: On the sliding of the glaciers, J. Glaciol., 3(21), 33–38, 1957.

van de Wel, N., Christoffersen, P. and Marion, B.: The influence of subglacial hydrology on the flow of Kamb Ice Stream, West Antarctica, J. Geophys. Res. Earth Surf., 118, 97–110, doi:10.1029/2012JF002570, 2013.

Wen, J., Wang, Y., Liu, J., Jezek, K., Huybrechts, P., Csatho, B., Farness, K. and Sun, B.: Mass budget of the grounded ice in the Lambert Glacier-Amery Ice Shelf system, Ann. Glaciol., 48, 193–197, 2008.

Werder, M., Hewitt, I., Schoof, C. and Flowers, G.: Modeling channelized and distributed subglacial drainage in two dimensions, J. Geophys. Res. Earth Surf., 118, 1–19, doi:10.1002/jgrf.20146, 2013.

Yang, S., Madsen, S., Rodehacke, C., Svendsen, S. and Aðalgeirsdóttir, G.: Modelling the Climate - Greenland Ice Sheet Interaction in the Coupled Ice-sheet/Climate Model EC-EARTH - PISM, 2014.

Yu, J., Liu, H., Jezek, K., Warner, R. and Wen, J.: Analysis of velocity field, mass balance, and basal melt of the Lambert Glacier–Amery Ice Shelf system by incorporating Radarsat SAR interferometry and ICESat laser altimetry measurements, J. Geophys. Res., 115(B11102), doi:10.1029/2010JB007456, 2010.

Zwally, J., Abdalati, W., Herring, T., Larson, K., Saba, J. and Steffen, K.: Surface Melt-Induced Acceleration of Greenland Ice-Sheet Flow, Science, 297(5579), 218–222, doi:10.1126/science.1072708, 2002.

Adams, M., Colella, P., Graves, D., Johnson, J., Johansen, H., Keen, N., Ligocki, T., Martin, D., McCorquodale, P., Modiano, D., Schwartz, P., Sternberg, T. and van Straalen, B.: Chombo software package for AMR applications – design document, [online] Available from: http://seesar.lbl.gov/anag/chombo/ChomboDesign-3.1.pdf, 2015.

Arthern, R. and Gudmundsson, H.: Initialization of ice-sheet forecasts viewed as an inverse Robin problem, J. Glaciol., 56, 527–533, doi:10.3189/002214310792447699, 2010.

Åström, J., Timo, R., Tallinen, T., Zwinger, T., Benn, D., Moore, J. and Timonen, J.: A particle based simulation model for glacier dynamics, The Cryosphere, 7, 1591–1602, doi:10.5194/tc-7-1591-2013, 2013.

Bamber, J. and Gomez-Dans, J. L.: The accuracy of digital elevation models of the Antarctic continent, Earth Planet. Sci. Lett., 237(3–4), 516–523, doi:10.1016/j.epsl.2005.06.008, 2005.

Benn, D. and Evans, D.: Glacier-climate interactions. In: Glaciers & Glaciation, 2nd ed., Routledge, Oxon, UK and New York, USA., 2010.

Benn, D. and Evans, D.: Glaciers and Glaciation, second., Routledge, Oxon, UK and New York, USA., 2013.

Borstad, C., Khazendar, A., Larour, E., Morlighem, M., Rignot, E., Schodlok, M. and Seroussi, H.: A damage mechanics assessment of the Larsen B ice shelf prior to collapse: Toward a physically-based calving law, Geophys. Res. Lett., 39(18), doi:10.1029/2012GL053317, 2012.

Broccoli, A. and Manabe, S.: The influence of continental ice, atmospheric CO2, and land albedo on the climate of the last glacial maximum, Clim. Dyn., 1(2), 87–99, doi:10.1007/BF01054478, 1987.

van den Broeke, M.: Momentum, Heat, and Moisture Budgets of the Katabatic Wind Layer over a Midlatitude Glacier in Summer, J. Appl. Meteorol., 36, 763–774, doi:10.1175/1520-0450(1997)036<0763:MHAMBO>2.0.CO;2, 1997.

Budd, W., Corry, M. and Jacka, T.: Results from the Amery Ice Shelf Project, Ann. Glaciol., 3, 36–41, doi:10.1017/S0260305500002494, 1982.

Christensen, O. B., Drews, M. and Christensen, J. H.: The HIRHAM Regional Climate Model Version 5 (beta), Technical Report, Danish Meteorological Institute. [online] Available from: http://www.dmi.dk/dmi/tr06-17, 2007.

Church, J., Clark, P., Cazenave, A., Gregory, J., Jevrejeva, S., Levermann, A., Merrifield, M., Milne, G., Nerem, S., Nunn, P., Payne, A., Pfeffer, T., Stammer, D. and Unnikrishnan, A.: Sea Level Change. In: Climate Change 2013: The Physical Science Basis. Contribution of Working Group I to the Fifth Assessment Report of the Intergovernmental Panel on Climate Change, Cambridge University Press, Cambridge, United Kingdom and New York, NY, USA., 2013.

Clark, C.: Glaciodynamic context of subglacial bedform generation and preservation, Ann. Glaciol., 28, 23–32, doi:10.3189/172756499781821832, 1999.

Cook, S., Rutt, I., Murray, T., Luckman, A., Zwinger, T., Sel, N., Goldsack, A. and James, T.: Modelling environmental influences on calving at Helheim Glacier in eastern Greenland, The Cryosphere, 8, 827–841, doi:10.5194/tc-8-827-2014, 2014.

Cornford, S., Martin, D., Graves, D., Ranken, G., Le Brocq, A., Gladstone, R., Payne, A., Ng, E. and Lipscomb, W.: Adaptive mesh, finite volume modeling of marine ice sheets, J. Comput. Phys., 232(1), 529–549, doi:10.1016/j.jcp.2012.08.037, 2013.

Cornford, S., Martin, D., Payne, A., Ng, E., Le Brocq, A., Gladstone, R., Edwards, T., Shannon, S., Agosta, C., van den Broeke, M., Hellmer, H., Krinner, G., Ligtenberg, S., Timmermann, R. and Vaughan, D.: Century-scale simulations of the response of the West Antarctic Ice Sheet to a warming climate, The Cryosphere, 9, 1579–1600, doi:10.5194/tc-9-1579-2015, 2015.

Cuffey, K. and Paterson, S.: The physics of the glaciers, fourth., Butterworth-Heinemann, Burlington, USA and Oxfrod, UK., 2010.

De Angelis, H. and Skvarca, P.: Glacier surge after ice shelf collapse, Science, 299(5612), 1560–1562, doi:10.1126/science.1077987, 2003.

Depooter, M., Bamber, J., Griggs, J., Lenaerts, J., Ligtenberg, S., van den Broeke, M. and Moholdt, G.: Calving fluxes and basal melt rates of Antarctic ice shelves, Nature, 502, 89–92, doi:10.1038/nature12567, 2013.

Dolgushin, L. ., Yevteyev, S. ., Krenke, A. ., Rototayev, K. . and Svatkov, N. .: The recent advance of the Medvezhiy Glacier, Prir. 1963, 11, 85–92, 1963.

Dowdeswell, J., Drewry, D. J., Cooper, A., Gorman, M., Liestol, O. and Orheim, O.: Digital mapping of the Nordaustlandet ice caps from airborne geophysical investigation, Ann. Glaciol., 8, 51–58, 1986.

Dowdeswell, J., Unwin, B., Nuttall, A. M. and Wingham, D.: Velocity structure, flow instability and mass flux on a large Arctic ice cap from satellite radar interferometry, Earth Planet. Sci. Lett., 167(3–4), 131–140, doi:10.1016/S0012-821X(99)00034-5, 1999.

Dowdeswell, J., Benham, T., Strozzi, T. and Hagen, J. O.: Iceberg calving flux and mass balance of the Austfonna ice cap onNordaustlandet, Svalbard, J. Geophys. Res., 113, doi:10.1029/2007JF000905, 2008.

Dunse, T., Greve, R., Schuler, T. V. and Hagen, J. O.: Permanent fast flow versus cyclic surge behaviour:numerical simulations of the Austfonna ice cap, Svalbard, J. Glaciol., 57, doi:10.3189/002214311796405979, 2011.

Dunse, T., Schellenberger, T., Hagen, J. O., Kääb, A., Schuler, T. V. and Reijmer, C.: Glacier-surge mechanisms promoted by a hydro-thermodynamic feedback to summer melt, The Cryosphere, 9, 197–215, doi:10.5194/tc-9-197-2015, 2015.

Eisen, O., Harrison, W., Raymond, C., Echelmeyer, K., Bender, G. and Gorda, J.: Variegated Glacier, Alaska, USA: A century of surges, J. Glaciol., 51(174), 399–406, doi:10.3189/172756505781829250, 2005.

Fowler, A., Murray, T. and Ng, F.: Thermally controlled glacier surging, J. Glaciol., 47, 527–538, 2001.

Frappé, T.-P. and Clark, G.: Slow surge of Trapridge Glacier, Yukon Territory, Canada, J. Geophys. Res. Earth Surf., 112(F3), doi:10.1029/2006JF000607, 2007.

Frey, P. and Alauzet, F.: Anisotropic mesh adaptation for CFD computations, Comput. Methods Appl. Mech. Eng., 194(48–49), 5068–5082, doi:10.1016/j.cma.2004.11.025, 2005.

Gagliardini, O., Cohen, D., Råback, P. and Zwinger, T.: Finite-element modeling of subglacial cavities and related friction law, J. Geophys. Res., 112, doi:10.1029/2006JF000576, 2007.

Gagliardini, O., Zwinger, T., Gillet-Chaulet, F., Durand, G., Favier, L., de Fleurian, B., Greve, R., Malinen, M., Martín, C., Råback, P., Ruokolainen, J., Sacchettini, M., Schäfer, M., Seddik, H. and Thies, J.: Capabilities and performance of Elmer/Ice, a new-generation ice sheet model, Geosci. Model Dev., 6, 1299–1318, doi:10.5194/gmd-6-1299-2013, 2013.

Galton-Fenzi, B., Hunter, J., Coleman, R., Marsland, S. and Warner, R.: Modeling the basal melting and marine ice accretion of the Amery Ice Shelf, J. Geophys. Res., 117(C9), doi:10.1029/2012JC008214, 2012.

Geuzaine, C. and Remacle, J.-F.: Gmsh: a three-dimensional finite element mesh generator with built-in pre- and post-processing facilities, Int. J. Numer. Methods Eng., 79(11), 1309–1331, doi:10.1002/nme.2579, 2009.

Gillet-Chaulet, F., Gagliardini, O., Seddik, H., Nodet, M., Durand, G., Ritz, C., Zwinger, T., Greve, R. and Vaughan, D.: Greenland ice sheet contribution to sea-level rise froma new-generation ice-sheet model, The Cryosphere, 6(6), 1561–1575, doi:10.5194/tc-6-1561-2012, 2012.

Gladstone, R., Lee, V., Vieli, A. and Payne, A.: Grounding line migration in an adaptive mesh ice sheet model, J. Geophys. Res. Earth Surf., 115(F4), doi:10.1029/2009JF001615, 2010.

Gladstone, R., Schäfer, M., Zwinger, T., Gong, Y., Strozzi, T., Mottram, R., Boberg, F. and Moore, J.: Importance of basal processes in simulations of a surging Svalbard outlet glacier, The Cryosphere, 8, 1393–1405, doi:10.5194/tc-8-1393-2014, 2014.

Glen, J.: The Creep of Polycrystalline Ice, Proc. R. Soc., 228(1175), 519–538, doi:10.1098/rspa.1955.0066, 1955.

Gong, Y., Zwinger, T., Gladstone, R., de Fleurian, B., Schäfer, M. and Moore, J.: Implementation of a hydrology model for Basin 3, Austfonna Ice Cap, Svalbard, 2014.

Helsen, M., van de Wal, R., van den Broeke, M., van de Berg, W. J. and Oerlemans, J.: Coupling of climate models and ice sheet models by surface massbalance gradients: application to the Greenland Ice Sheet, The Cryosphere, 6, 255–272, doi:10.5194/tc-6-255-2012, 2012.

Hindmarsh, R.: Deforming beds: viscous and plastic scales of deformation, Quat. Sci. Rev., 16(9), 1039–1056, doi:10.1016/S0277-3791(97)00035-8, 1997.

Holt, J., Blankenship, D., Morse, D., Young, D., Peters, M., Kempf, S., Richter, T., Vaughan, D. and Corr, H.: New boundary conditions for the West Antarctic Ice Sheet: Subglacial topography of the Thwaites and Smith glacier catchments, Geophys. Res. Lett., 33(L09502), doi:10.1029/2005GL025561, 2006.

Hooke, R.: Flow law for polycrystalline ice in glaciers: Comparison of theoretical predictions, laboratory data, and field measurements, Rev. Geophys., 19(4), 664–672, doi:10.1029/RG019i004p00664, 1981.

Hourdin, F., Musat, I., Bony, S., Braconnot, P., Codron, F., Dufresne, J.-L., Fairhead, L., Filiberti, M.-A., Friedlingstein, P., Grandpeix, J.-Y., Krinner, G., LeVan, P., Li, Z. and Lott, F.: The LMDZ4 general circulation model: climate performance and sensitivity to parametrized physics with emphasis on tropical convection, Clim. Dyn., 27, 787–813, doi:10.1007/s00382-006-0158-0, 2006.

Iverson, N., Hooyer, T. and Baker, R.: Ring-shear studies of till deformation: Coulomb plastic behaviour and distributed strain in glacier beds, J. Glaciol., 44, 634–642, doi:10.1017/S0022143000002136, 1998.

Jakobsson, M., Macnab, R., Mayer, L., Anderson, R., Edwards, M., Hatzky, J., Schenke, H. W. and Johnson, P.: An improved bathymetric portrayal of the Arctic Ocean: Implications for ocean modeling and geological, geophysical and oceanographic analyses, Geophys. Res. Lett., 35, doi:10.1029/2008GL033520, 2008.

Jezek, K., Farness, K., Carande, R., Wu, X. and Labelle-Hamer, N.: RADARSAT 1 synthetic aperture radar observations of Antarctica: Modified Antarctic Mapping Mission, 2000, Radio Sci., 38(4), doi:10.1029/2002RS002643, 2003.

Joughin, I., Tulaczyk, S., Bamber, J., Blankenship, D., Holt, J., Scambos, T. and Vaughan, D.: Basal conditions for Pine Island and Thwaites Glaciers, West Antarctica, determined using satellite and airborne data, J. Glaciol., 55(190), 245–257, 2009.

Kamb, B.: Sliding motion of glaciers: theory and observation, Rev. Geophys., 8(4), 673–728, doi:10.1029/RG008i004p00673, 1970.

Kamb, B.: Rheological nonlinearity and flow instability in the deforming bed mechanism of ice stream motion, J. Geophys. Res., 96, 16585–16595, doi:10.1029/91JB00946, 1991.

Kamb, B., Raymond, C., Harrison, W., Engelhardt, H., Echelmeyer, K., Humphrey, N., Brugman, M. and Pfeffer, T.: Glacier Surge Mechanism: 1982-1983 Surge of Variegated Glacier, Alaska, Science, 227(4686), 469–479, doi:10.1126/science.227.4686.469, 1985.

Langen, P., Mottram, R., Christensen, J., Boberg, F., Rodehacke, C., Stendel, M., van As, D., Ahlstrøm, A., Mortensen, J., Rysgaard, S., Petersen, D., Svendsen, K., Aðalgeirsdóttir, G. and Cappelen, J.: Estimating and understanding recent changes in the energy and freshwater budget for Godthåbsfjord catchment with a 5 km regional climate model, Prep., 2014.

Le Brocq, A., Payne, A. and Vieli, A.: An improved Antarctic dataset for high resolution numerical ice sheet models (ALBMAP v1), Earth Syst. Sci. Data, 2, 247–260, doi:5194/essd-2-247-2010, 2010.

Liu, Y., John, M., Cheng, X., Gladstone, R., Bassis, J., Liu, H., Wen, J. and Hui, F.: Ocean-driven thinning enhances iceberg calving and retreat of Antarctic ice shelves, Proc. Natl. Acad. Sci., 112(11), 3263–3268, doi:10.1073/pnas.1415137112, 2015.

Lliboutry, L.: Realistic, yet simple bottom boundary conditions for glaciers and ice sheets, J. Geophys. Res. Solid Earth, 92(B9), 9101–9109, doi:10.1029/JB092iB09p09101, 1987.

Luckman, A., Murray, T. and Strozzi, T.: Surface flow evolution throughout a surge measured by satellite radar interferometry, Geophys. Res. Lett., 29, doi:10.1029/2001GL014570, 2002.

Lythe, M., Vaughan, D. and the BEDMAP Consortium: A new ice thickness and subglacial topographic model of Antarctica, J. Geophys. Res., 106(B6), 11335–11351, doi:10.1029/2000JB900449, 2001.

Ma, Y., Gagliardini, O., Ritz, C., Gillet-Chaulet, F., Durand, G. and Montagnat, M.: Enhancement factors for grounded ice and ice shelves inferred from an anisotropic ice-flow model, J. Glaciol., 56, 805–812, doi:10.3189/002214310794457209, 2010.

MacAyeal, D.: A tutorial on the use of control methods in ice sheet modeling, J. Glaciol., 39, 91–98, 1993.

Macheret, Y. and Vasilenko, E.: Pecularities of internal structure and regime of glaciers on Nordaustlandet by airborne radio-echo sounding data (In Russian with English summary), Data Glaciol. Stud., 62, 44–56, 1988.

Marsland, S., Haak, H., Jungclaus, J., Latif, M. and Röske, F.: The Max-Planck-Institute global ocean/sea ice model with orthogonal curvilinear coordinates, Ocean Model., 5(2), 91–127, 2003.

Martin, D., Colella, P. and Graves, D.: A cell-centered adaptive projection method for the incompressible Navier–Stokes equations in three dimensions, J. Comput. Phys., 227(3), 1863–1886, doi:10.1016/j.jcp.2007.09.032, 2008.

McMillan, M., Shepherd, A., Gourmelen, N., Dehecq, A., Leeson, A., Ridout, A., Flament, T., Hogg, A., Gilbert, L., Benham, T., Michiel van den Broeke, Julian Dowdeswell, Xavier Fettweis, Brice Noël and Tazio Strozzi: Rapid dynamic activation of a marine-basedArctic ice cap, Geophys. Res. Lett., 41, 8902–8909, doi:10.1002/2014GL062255, 2014.

Meier, M. and Post, A.: What are glacier surges?, Can. J. Earth Sci., 6(4), 807–817, doi:10.1139/e69-081, 1969.

van Meijgaard, E., van Ulft, B., van de Berg, W. J., Bosveld, F., van den Hurk, B., Lenderink, G. and Siebesma, P.: The KNMI regional atmospheric climate model RACMO, version 2.1, Technical Report, Royal Netherlands Meteorological Institute, De Bilt., 2008.

Mercer, J.: West Antarctic ice sheet and CO2 greenhouse effect: a threat of disaster, Nature, 271, 321–325, doi:10.1038/271321a0, 1978.

Moholdt, G. and Kääb, A.: A new DEM of the Austfonna ice capby combining differential SAR interferometry with ICESat laseraltimetry, Polar Res., 31, doi:10.3402/polar.v31i0.18460, 2012.

Moholdt, G., Hagen, J. O., Eiken, T. and Schuler, T. V.: Geometric changes and mass balance of the Austfonna ice cap,Svalbard, The Cryosphere, 4, 21–34, doi:10.5194/tc-4-21-2010, 2010.

Morlighem, M., Rignot, E., Seroussi, H., Larour, E., Ben Dhia, H. and Aubry, D.: Spatial patterns of basal drag inferred using control methods from a full-Stokes and simpler models for Pine Island Glacier, West Antarctica, Geophys. Res. Lett., 37, doi:10.1029/2010GL043853, 2010.

Murray, T., Strozzi, T., Luckman, A., Jiskoot, H. and Christakos, P.: Is there a single surge mechanism? Contrasts in dynamics betweenglacier surges in Svalbard and other regions, J. Geophys. Res., 108(B5), 2237, doi:10.1029/2002JB001906, 2003.

Nick, F., van de Veen, C. J., Vieli, A. and Benn, D.: A physically based calving model applied to marine outlet glaciers and implications for the glacier dynamics, J. Glaciol., 56, 781–794, doi:10.3189/002214310794457344, 2010.

Nick, F., Vieli, A., Andersen, M., Joughin, I., Payne, A., Edwards, T., Pattyn, F. and van de Wal, R.: Future sea-level rise from Greenland's main outlet glaciers in a warming climate, Nature, 497, 235–238, doi:10.1038/nature12068, 2013.

Nye, J.: The Distribution of Stress and Velocity in Glaciers and Ice-Sheets, Proc. R. Soc., 239(1216), 113–133, doi:10.1098/rspa.1957.0026, 1957.

Pattyn, F., Perichon, L., Durand, G., Favier, L., Gagliardini, O., Hindmarsh, R., Zwinger, T., Albrecht, T., Cornford, S., Docquier, D., Fürst, J., Goldberg, D., Gudmundsson, H., Humbert, A., Hütten, M., Huybrechts, P., Jouvet, G., Kleiner, T., Larour, E., Martin, D., Morlighem, M., Payne, A., Pollard, D., Rückamp, M., Rybak, O., Seroussi, H., Thoma, M. and Wilkens, N.: Grounding-line migration in plan-view marine ice-sheet models: results of the ice2sea MISMIP3d intercomparison, J. Glaciol., 59, 410–422, doi:10.3189/2013JoG12J129, 2013.

Pfirman, S. and Solheim, A.: Subglacial meltwater discharge in the open-marine tidewater glacier environment: observations from Nordaustlandet, Svalbard Archipelago, Mar. Geol., 86(4), 265–281, 1989.

Phillips, T., Rajaram, H. and Steffen, K.: Cryo-hydrologic warming: A potential mechanism for rapid thermal response of ice sheets, Geophys. Res. Lett., 37, doi:10.1029/2010GL044397, 2010.

Pohjola, V., Christoffersen, P., Kolondra, L., Moore, J., Pettersson, R., Schäfer, M., Strozzi, T. and Reijmer, C.: Spatial distribution and change in the surface ice-velocity field of Vestfonna ice cap, Nordaustlandet, Svalbard, 1995–2010 usinggeodetic and satellite interferometry data, Geogr. Ann. Ser. Phys. Geogr., 93, 323–335, doi:10.1111/j.1468-0459.2011.00441.x, 2011.

Pope, V., Gallani, M., Rowntree, P. and Stratton, R.: The impact of new physical parametrizations in the Hadley Centre climate model: HadAM3, Clim. Dyn., 16(2–3), 123–146, doi:10.1007/s003820050009, 2000.

Rae, J., Aðalgeirsdóttir, G., Edwards, T., Fettweis, X., Gregory, J., Hewitt, H., Lowe, J., Lucas-Picher, P., Mottram, R., Payne, A., Ridley, J., Shannon, S., van de Berg, W., van de Wal, R. and van de Broeke, M.: Greenland ice sheet surface mass balance: evaluating simulations and making projections with regional climate models, The Cryosphere, 6, 1275–1294, doi:10.5194/tc-6-1275-2012, 2012.

Rignot, E., Bamber, J., van den Broeke, M., Davis, C., Li, Y., van de Berg, W. J. and van Meijgaard, E.: Recent Antarctic ice mass loss from radar interferometry and regional climate modelling, Nat. Geosci., 1, 106–110, doi:10.1038/ngeo102, 2008.

Rignot, E., Mouginot, J. and sch, B.: Ice Flow of the Antarctic Ice Sheet, Science, 333(6048), 1427–1430, doi:10.1126/science.1208336, 2011.

Roeckner, E., Bäuml, G., Bonaventura, L., Brokopf, R., Esch, M., Giorgetta, M., Schlese, U., Schulzweida, U., Kirchner, I., Manzini, E., Rhodin, A. and Tompkins, A.: The atmospheric general circulation model ECHAM 5. Part I: Model description, Max-Planck-Institut für Meteorologie, Hamburg, Germany., 2003.

Rott, H., Rack, W., Skvarca, P. and De Angelis, H.: Northen Larsen Ice Shelf, Antarctica: further retreat after collapse., Ann. Glaciol., 34, 277–282, doi:10.3189/172756402781817716, 2002.

Sanderson, T.: Equilibrium profile of ice shelves, J. Glaciol., 22, 435–460, 1979.

Scambos, T., Haran, T., Fahnestock, M., Painter, T. and Bohlander, J.: MODIS-based Mosaic of Antarctica (MOA) data sets: Continent-wide surface morphology and snow grain size, Remote Sens. Environ., 111(2–3), 242–257, doi:10.1016/j.rse.2006.12.020, 2007.

Schäfer, M., Möller, M., Zwinger, T. and Moore, J.: Dynamic modelling of future glacier changes: mass balance/elevation feedback in projections for the Vestfonna ice cap, Nordaustlandet, Svalbard, J. Glaciol., 61, 1121–1136, doi:10.3189/2015JoG14J184, 2015.

Schellenberger, T., Dunse, T., Kääb, A., Schuler, T. V., Hagen, J. O. and Reijmer, C.: Multi-year surface velocities and sea-level rise contribution of the Basin-3 and Basin-2 surges, Austfonna, Svalbard, Cryosphere Discuss, doi:10.5194/tc-2017-5, 2017.

Schoof, C.: The effect of cavitation on glacier sliding, Proceeding R. Soc. A, 461, 609–627, doi:10.1098/rspa.2004.1350, 2005.

Schoof, C.: Ice sheet grounding line dynamics: steady states, stability and hysteresis, J. Geophys. Res. Earth Surf., 112, doi:10.1029/2006JF000664, 2007.

Schoof, C. and Hindmarsh, R.: Thin-Film Flows with Wall Slip: An Asymptotic Analysis of Higher Order Glacier Flow Models, Q. J. Mech. Appl. Math., 63, 73–114, doi:10.1093/qjmam/hbp025, 2010.

Sharp, M.: Surging glaciers: behaviour and mechanisms, Prog. Phys. Geogr., 12(3), 349–370, 1988.

Solheim, A. and Pfirman, S.: Sea-floor morphology outside a grounded, surging glacier - Bråsvellbreen,Svalbard, Mar. Geol., 65(1–2), 127–143, 1985.

Sun, S., Cornford, S., Gwyther, D., Gladstone, R., Galton-Fenzi, B., Zhao, L. and Moore, J.: Impact of ocean forcing on the Aurora Basin in the 21st and 22nd centuries, Ann. Glaciol., 57(73), 1–8, doi:10.1017/aog.2016.27, 2016.

Taurisano, A., Schuler, T. V., Hagen, J. O., Eiken, T., Loe, E., Melvold, K. and kohler, J.: The distribution of snow accumulation across the Austfonna ice cap, Svalbard: direct measurements and modelling, Polar Res., 26, 7–13, doi:10.1111/j.1751-8369.2007.00004.x, 2007.

Undén, P., Rontu, L., Järvinen, H., Lynch, P., Calvo, J., Cats, G., Cuxart, J., Eerola, K., Fortelius, C., Garcia-Moya, J., Jones, C., Lenderink, G., McDonald, A., McGrath, R., Navascues, B., Nielsen, N., _degaard, V., Rodriguez, E., Rummukainen, M., Room, R., Sattler, K., Sass, B., Savijärvi, H., Schreur, B., Sigg, R., The, H. and Tijm, A.: HIRLAM-5 Scientific Documentation, [online] Available from: http://hirlam.org, 2002.

Vasilenko, E., Navarro, F., Dunse, T., Eiken, T. and Hagen, J. O.: New low-frequency radio-echo soundings of Austfonna Ice Cap, Svalbard, in The Dynamics and Mass Budget of Arctic Glaciers. Extended abstracts, Canada., 2009.

Vaughan, D., Corr, H., Ferraccioli, F., Frearson, N., O'Hare, A., Mach, D., Holt, J., Blankenship, D., Morse, D. and Young, D.: New boundary conditions for the West Antarctic ice sheet: subglacial topography beneath Pine Island Glacier, Geophys. Res. Lett., 33(L09501), doi:10.1029/2005GL025588, 2006.

Vaughan, D., Comiso, J., Allison, I., Carrasco, J., Kaser, G., Kwok, R., Mote, P., Murray, T., Paul, F., Ren, J., Rignot, E., Solomina, O., Steffen, K. and Zhang, T.: Observations: Cryosphere. In: Climate Change 2013: The Physical Science Basis. Contribution of Working Group I to the Fifth Assessment Report of the Intergovernmental Panel on Climate Change, Cambridge University Press, Cambridge, United Kingdom and New York, NY, USA., 2013.

Vieli, A., Payne, A., Du, Z. and Shepherd, A.: Numerical modelling and data assimilation of the Larsen B ice shelf, Antarctic Peninsula, Philos. Trans. R. Soc. Math. Phys. Eng. Sci., 15, 1815–1839, doi:10.1098/rsta.2006.1800, 2006.

van de Wal, R., Boot, W., van den Broeke, M., Smeets, P., Reijmer, C., Donker, J. and Oerlemans, J.: Large and Rapid Melt-InducedVelocity Changes in the AblationZone of the Greenland Ice Sheet, Science, 321(5885), 111–113, doi:10.1126/science.1158540, 2008.

Wang, enli, Annette, R., John, M., Xuefeng, C., Duoying, J., Q, L., N, Z., Chenghai, W., Shiqiang, Z., David, L., Dave, U. G. S., Wenxin, Z., Christine, D., Charles, K., Kazuyuki, S., Andrew, M., Eleanor, B. and B, D.: Diagnostic and model dependent uncertainty of simulated Tibetan permafrost area, The Cryosphere, 10, 287–306, doi:10.5194/tc-10-287-2016, 2016.

Wang, Q., Danilov, S., Sidorenko, D., Timmermann, R., Wekerle, C., Wang, X., Jung, T. and Schröter, J.: The Finite Element Sea Ice-Ocean Model (FESOM) v.1.4: Formulation of an ocean general circulation model, Geosci. Model Dev., 7, 663–693, doi:10.5194/gmd-7-663-2014, 2014.

Weertman, J.: On the sliding of the glaciers, J. Glaciol., 3(21), 33–38, 1957.

van de Wel, N., Christoffersen, P. and Marion, B.: The influence of subglacial hydrology on the flow of Kamb Ice Stream, West Antarctica, J. Geophys. Res. Earth Surf., 118, 97–110, doi:10.1029/2012JF002570, 2013.

Wen, J., Wang, Y., Liu, J., Jezek, K., Huybrechts, P., Csatho, B., Farness, K. and Sun, B.: Mass budget of the grounded ice in the Lambert Glacier-Amery Ice Shelf system, Ann. Glaciol., 48, 193–197, 2008.

Werder, M., Hewitt, I., Schoof, C. and Flowers, G.: Modeling channelized and distributed subglacial drainage in two dimensions, J. Geophys. Res. Earth Surf., 118, 1–19, doi:10.1002/jgrf.20146, 2013.

Yang, S., Madsen, S., Rodehacke, C., Svendsen, S. and Aðalgeirsdóttir, G.: Modelling the Climate - Greenland Ice Sheet Interaction in the Coupled Ice-sheet/Climate Model EC-EARTH - PISM, 2014.

Yu, J., Liu, H., Jezek, K., Warner, R. and Wen, J.: Analysis of velocity field, mass balance, and basal melt of the Lambert Glacier–Amery Ice Shelf system by incorporating Radarsat SAR interferometry and ICESat laser altimetry measurements, J. Geophys. Res., 115(B11102), doi:10.1029/2010JB007456, 2010.

Zwally, J., Abdalati, W., Herring, T., Larson, K., Saba, J. and Steffen, K.: Surface Melt-Induced Acceleration of Greenland Ice-Sheet Flow, Science, 297(5579), 218–222, doi:10.1126/science.1072708, 2002.

Part II
Journal Publications